Mixing of parity of a nucleon pair at the nuclear surface due to the spin-orbit potential in ^{18}F

Yoshiko Kanada-En'yo
Department of Physics, Kyoto University, Kyoto 606-8502, Japan

Fumiharu Kobayashi
Department of Physics, Niigata University, Niigata 950-2181, Japan

(Received 1 July 2014; revised manuscript received 12 October 2014; published 21 November 2014)

We investigate the structure of ^{18}F with the microscopic wave function based on the three-body $^{16}\mathrm{O}+p+n$ model. In the calculation of the generator coordinate method of the three-body model, $T=0$ energy spectra of $J^\pi = 1^+$, 3^+, and 5^+ states and $T=1$ spectra of $J^\pi = 0^+$, 2^+ states in ^{18}F are described reasonably. Based on the dinucleon picture, the effect of the spin-orbit force on the $T=0$ and $T=1$ pn pairs around the ^{16}O core is discussed. The $T=1$ pair in the $J^\pi = 0^+$ state gains the spin-orbit potential energy involving the odd-parity mixing in the pair. The spin-orbit potential energy gain with the parity mixing is not so efficient for the $T=0$ pair in the $J^\pi = 1^+$ state. The parity mixing in the pair is regarded as the internal symmetry breaking of the pair in the spin-orbit potential at the nuclear surface.

DOI: 10.1103/PhysRevC.90.054332 PACS number(s): 21.10.−k, 21.30.Fe, 21.60.Gx

I. INTRODUCTION

Motivated by the progress of experimental research on unstable nuclei, the interest in proton and neutron (pn) pair correlations has been revived in recent years, and pn pairing in proton-rich nuclei near the $Z=N$ line has been intensively investigated. The importance of the pn pairing has been discussed for a long time (see Refs. [1–3] and references therein). In the recent studies of the pn pairing, the competition between isoscalar $T=0$ pairing and isovector $T=1$ pairing has been attracting a great interest. Moreover, the possibility of the $T=0$ and $T=1$ mixed pairing has been studied with the recently developed mean-field approaches including isospin mixing [4–6]. The pn pairing also has been discussed in relation with the Wigner energy in even-even nuclei, and more explicitly, its role in four-nucleon α-like correlations has been investigated in recent works [7,8].

The competition between $T=0$ pairing and $T=1$ pairing is one of the essential problems in $Z\sim N$ nuclei. As is well known, the nuclear interaction in free space is more attractive in the $T=0$ spin-triplet even (^{3}E) channel than in the $T=1$ spin-singlet even (^{1}E) channel, as shown by the fact that the $T=0$ pn system forms a bound state, a deuteron. Because the $T=0$ interaction is considered to be stronger than the $T=1$ interaction also in nuclear medium and at the nuclear surface, it is expected naively that the deuteronlike $T=0$ pair is more favored than the $T=1$ pair. Nevertheless, as seen in the ground-state spins of the odd-odd nuclei, the $T=1$ pairing is often favored over the $T=0$ pairing except for light nuclei [9]. Many theoretical calculations have been achieved to investigate the competition between the $T=0$ and $T=1$ pairing and suggested that the $T=1$ pairing rather than the $T=0$ pairing occurs in the ground states of many $Z=N$ medium-mass nuclei [5,10–17]. The origin of the suppression of the $T=0$ pairing has been discussed from the standpoint of the coupling of single-particle angular momenta, and the important role of the spin-orbit force in the $T=0$ and $T=1$ pair competition has been pointed out [5,12,15–18]. Namely, the spin-orbit potential tends to suppress more the $T=0$, $J=1$ pairing than the $T=1$, $J=0$ pairing because the S-wave component of the relative motion between two nucleons in the j^2 configuration is much smaller for the $T=0$, $J=1$ pair than for the $T=1$, $J=0$ pair.

However, it has been theoretically suggested that, in rotational states, the $T=0$ pairing is more favored than the $T=1$ pairing in the high-spin region [19–24]. Recently, a spin-aligned pn pair in medium-mass $N=Z$ nuclei has been reported in the experimental work [25], which has stimulated the subsequent theoretical studies [26,27].

The trend of the pn pairing condensation can be understood by the feature of one pn pair. That is, a $T=0$ pn pair is suppressed in low-spin states, while it can persist in a rotating system. In the recent work by Tanimura *et al.* [28], the pn correlation in a single pair around a core has been systematically studied within the three-body potential model calculation, and it has been shown that the spin-orbit potential plays an important role in the suppression of the pn pair in the $T=0$, $J^\pi = 1^+$ state. It means that the properties of a pn pair around a core reflects the basic feature of the pn correlation, and the study of one pn pair can be helpful to understand the pn pairing phenomena in nuclei.

Our aim is to investigate features of a pn pair around a core nucleus and clarify the mechanism how the spin-orbit field affects the pn pair. In the present work, we discuss the effect of the spin-orbit force from the standpoint of the two-nucleon cluster (dinucleon) picture. A proton and a neutron bound in the potential from the core nucleus are expected to form a deuteronlike $T=0$ pair at the nuclear surface because of the nucleon-nucleon attraction in the ^{3}E channel. Similarly to the $T=0$ pair, because of the ^{1}E attraction a proton and a neutron may also form a $T=1$ pair, which is the analog state of the nn pair in a system of two neutrons around a core. The $T=0$ and $T=1$ pn pairs are not necessarily the same as the two-nucleon (quasi)bound states in free space, but the pair called dinucleon is regarded as a virtual bound state of spatially correlating two nucleons confined in the central potential from the core.

In the central potential without the spin-orbit potential, the lowest $T=0$ and $T=1$ states of two nucleons are the pure

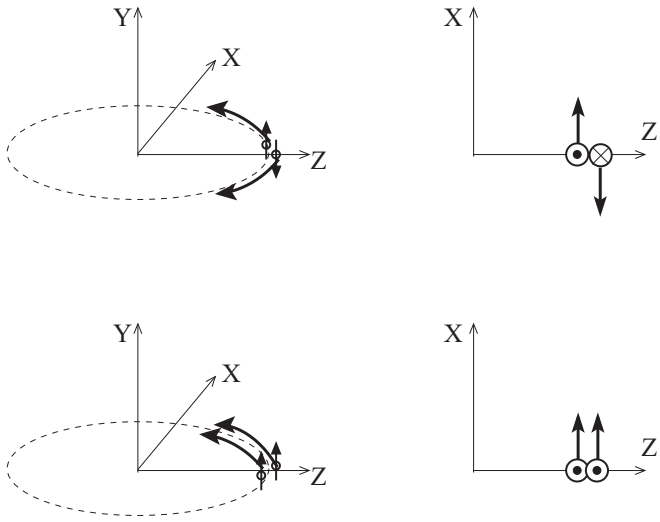

FIG. 1. Schematic figures for two nucleons in the pair in the spin-orbit potential at the nuclear surface. The effect of the spin-orbit field on the $\uparrow_Y\downarrow_Y$ pn pair (the opposite boost in the antiparallel-spin pair) and that on the $\uparrow_Y\uparrow_Y$ pn pair (the rotation boost of the parallel-spin pair) in the body-fixed frame XYZ are shown in the top and bottom panels, respectively.

even-parity $(TS) = (01)$ and $(TS) = (10)$ states without the odd-parity mixing because the Hamiltonian for two nucleons is invariant with respect to the exchange of the coordinates of nucleons $\boldsymbol{r}_1 \leftrightarrow \boldsymbol{r}_2$ in the pair and conserves the internal parity of the pair. Then, considering the spin-orbit potential as a perturbative field, we discuss how the $T = 0$ and $T = 1$ pn pairs are affected by the external perturbative field. This dinucleon picture is different from the usual mean-field picture in the jj coupling scheme, in which the central and spin-orbit potentials are considered to be unperturbative fields and pair correlations are caused by the residual pn interaction (see Appendix A).

The present work is based on the following idea in the dinucleon picture. Suppose that two nucleons in the $(TS) = (01)$ pair located at a position on the Z axis have intrinsic spins oriented to the Y axis, as shown in bottom panels of Fig. 1. When the perturbative field of the spin-orbit potential is imposed, two nucleons in the pair are boosted to have finite momenta along the X axis, i.e., the finite orbital angular momenta around the core so as to gain the spin-orbit potential energy. The boosting of two nucleons in the same direction does not change the internal structure of the pair but it causes the rotation of the center-of-mass (c.m.) motion of the pair around the core. It means that high-spin states gain the spin-orbit potential energy without the internal energy loss of the pair, while the zero orbital angular momentum $L = 0$ state cannot gain the spin-orbit potential. Thus, the dinucleon picture provides a simple interpretation for the reason why the $T = 0$ pn pair can persist in a rotating system although the $T = 0$ pn pair may be relatively unfavored by the spin-orbit force in the low-spin state.

Moreover, we find further interesting phenomenon of the symmetry breaking, that is, the parity mixing in the $T = 1$ pn pair. Suppose that two nucleons in the $(TS) = (10)$ pair have antiparallel intrinsic spins oriented to the Y axis as shown in the top panels of Fig. 1. In the potential with the spin-orbit field, the internal parity symmetry is explicitly broken because the spin-orbit potential is not invariant with respect to $\boldsymbol{r}_1 \leftrightarrow \boldsymbol{r}_2$ for the spin-up and -down nucleons in the pair. Two nucleons in the pair are boosted along the X axis in the opposite direction so as to gain the spin-orbit potential energy. As a result of the opposite boost, the parity mixing of the $(TS) = (10)$ and (11) occurs in the $T = 1$ pair. In other words, the role of the spin-orbit force on the $T = 1$ pair is the internal parity mixing owing to the opposite boost of antiparallel-spin nucleons in the pair ("opposite boost" in the pair), while that on the $T = 0$ pair of parallel-spin nucleons is "rotation boost" of the pair for high L states.

Similar phenomenon of parity mixing of pairs has been discussed recently in the condensed-matter physics [29]. The parity mixing of Cooper pairs has been suggested to occur because of the spin-orbit interaction in noncentrosymmetric superconductors having the breaking of inversion symmetry in the crystal structure. The mechanism of the parity mixing is analogous to that of the two-nucleon pair caused by the spin-orbit field at the nuclear surface.

In this paper, we investigate the structure of ^{18}F with the microscopic wave function based on a three-body $^{16}\mathrm{O} + p + n$ model and discuss the behavior of the pn pair around ^{16}O. In the present model, two nucleons are treated as Gaussian wave packets around ^{16}O, which is assumed to be the inert core written by the harmonic oscillator (H.O.) p-shell closed configuration. The antisymmetrization between 18 nucleons and the recoil effect of the core are exactly taken into account, and the energy spectra of ^{18}F are calculated using phenomenological effective nuclear forces. In that sense, the ^{18}F wave function used in the present work is a fully microscopic one. One of the advantages of the present model is that the expression of the Gaussian wave packets for valence nucleon wave functions provides the direct link with the $(0s)^2$ pn cluster formation and its breaking at the nuclear surface. Moreover, the internal wave function and the c.m. motion of the pair are separable. It is also helpful to consider a classical picture for the position and momentum of valence nucleons in the pair. Based on the dinucleon picture, we analyze the effect of the spin-orbit potential on the pn pair around the ^{16}O core and discuss the parity mixing of the pn pair considering the spin-orbit potential from the core as the perturbative external field. We also discuss the effect of the spin-orbit potential on the four-nucleon correlations, i.e., the breaking of the α cluster around ^{16}O in association with that on the pn pair.

This paper is organized as follows. In the next section, we describe the present model of the microscopic three-body $^{16}\mathrm{O} + p + n$ model. In Sec. III, the calculated results for ^{18}F obtained by the GCM calculations of the $^{16}\mathrm{O} + p + n$ model are shown. We discuss the behavior of the pn pair focusing on the effect of the spin-orbit potential in Sec. IV. We also study the four-nucleon correlation at the surface of the ^{16}O core based on the $^{16}\mathrm{O} + ppnn$ model in Sec. V. A summary is given in Sec. VI. In the appendixes, the mechanism of the breaking of the parity symmetry in the pair in the spin-orbit potential is described in Appendix A, and the mathematical relation between the pn cluster wave function and the shell-model wave function is described in Appendix B.

II. FORMULATION

To investigate the structure of ^{18}F system focusing on the internal structure of the pn pair at the surface around the ^{16}O core, we adopt a three-body cluster model of $^{16}\mathrm{O}+p+n$ with the form of Gaussian wave packets for two valence nucleons,

$$\Phi_{^{16}\mathrm{O}+pn}(\boldsymbol{R}_1,\boldsymbol{R}_2)=\mathcal{A}\{\Phi_{^{16}\mathrm{O}}\psi_{p\sigma}(\boldsymbol{R}_1)\psi_{n\sigma'}(\boldsymbol{R}_2)\}, \quad (1)$$

$$\psi_{\tau\sigma}(\boldsymbol{R}_j;\boldsymbol{r}_i)=\phi(\boldsymbol{R}_j;\boldsymbol{r}_i)\chi_{\tau\sigma}, \quad (2)$$

$$\phi(\boldsymbol{R}_j;\boldsymbol{r}_i)=\left(\frac{2\nu}{\pi}\right)^{3/4}e^{-\nu(\boldsymbol{r}_i-\boldsymbol{R}_j)^2}. \quad (3)$$

Here $\Phi_{^{16}\mathrm{O}}$ is the ^{16}O wave function given by the H.O. p-shell closed configuration with the width $b=1/\sqrt{2\nu}$ fixed to be $\nu=0.16$ fm^{-2} to reproduce the root-mean-square radius of ^{16}O. In the practical calculation, $\Phi_{^{16}\mathrm{O}}$ is approximately written by the 4α Brink-Bloch wave function with the α-α distance small enough to express the shell-model limit. $\chi_{\tau\sigma}$ is the spin-isospin function labeled by $\tau=$ proton or neutron and $\sigma=\uparrow$ or $\downarrow$, and $\mathcal{A}$ is the antisymmetrizer for all nucleons. The total wave function is the microscopic 18-body wave function. The spatial parts of single-particle wave functions for valence nucleons are specified by the complex parameters $\boldsymbol{R}_j$ ($j=1,2$), which stand for the centers of Gaussian wave packets in the phase space. One of the merits of the present model with the wave-packet form is that the internal wave function and the c.m. motion of the pair are separable,

$$\phi(\boldsymbol{R}_1;\boldsymbol{r}_1)\phi(\boldsymbol{R}_2;\boldsymbol{r}_2)=\phi_g(\boldsymbol{R}_g;\boldsymbol{r}_g)\phi_{\mathrm{in}}(\boldsymbol{R};\boldsymbol{r}), \quad (4)$$

$$\phi_g(\boldsymbol{R}_g;\boldsymbol{r}_g)=\left(\frac{4\nu}{\pi}\right)^{3/4}e^{-2\nu(\boldsymbol{r}_g-\boldsymbol{R}_g)^2}, \quad (5)$$

$$\phi_{\mathrm{in}}(\boldsymbol{R};\boldsymbol{r})=\left(\frac{\nu}{\pi}\right)^{3/4}e^{-\frac{\nu}{2}(\boldsymbol{r}-\boldsymbol{R})^2}, \quad (6)$$

$$\boldsymbol{R}_g=\frac{\boldsymbol{R}_1+\boldsymbol{R}_2}{2}, \quad \boldsymbol{R}=\boldsymbol{R}_1-\boldsymbol{R}_2, \quad (7)$$

and, therefore, the internal structure of the pair can be easily analyzed if we omit the antisymmetrization effect from the core. Moreover, the recoil effect on the core is exactly taken into account by shifting $\boldsymbol{R}_{1,2}\to\boldsymbol{R}_{1,2}-\boldsymbol{R}_g/9$ and also the mean position of the c.m. of ^{16}O to $-\boldsymbol{R}_g/9$. Note that the valence nucleon wave function given by the localized Gaussian form can be expanded by the H.O. shell-model basis around the origin and, in the $|\boldsymbol{R}_j|\to 0$ limit, the single-nucleon wave function after the antisymmetrization becomes equivalent to a H.O. sd orbit around the ^{16}O core, as explained in Appendix B. By transforming the one-center coordinates $\boldsymbol{r}_1$ and $\boldsymbol{r}_2$ to the Jaccobi coordinates $\boldsymbol{r}$ and $\boldsymbol{r}_g$, we can switch over from the single-particle orbit picture to the pn cluster picture.

Another merit of the wave-packet form is that the mean position and momentum of a nucleon are described simply by the real part $\boldsymbol{d}_j$ and the imaginary part $\boldsymbol{k}_j/2\nu$ of the Gaussian center parameter $\boldsymbol{R}_j=\boldsymbol{d}_j+i\boldsymbol{k}_j/2\nu$ ($\boldsymbol{d}_j$ and $\boldsymbol{k}_j$ are real vectors),

$$\langle\phi(\boldsymbol{R}_j)|\boldsymbol{r}_i|\phi(\boldsymbol{R}_j)\rangle=\boldsymbol{d}_j, \quad (8)$$

$$\langle\phi(\boldsymbol{R}_j)|\boldsymbol{p}_i|\phi(\boldsymbol{R}_j)\rangle=\hbar\boldsymbol{k}_j, \quad (9)$$

and also those for the c.m. of the pn pair,

$$\boldsymbol{R}_g=\boldsymbol{D}_g+i\boldsymbol{K}_g/4\nu, \quad (10)$$

$$\boldsymbol{D}_g=\langle\phi_g(\boldsymbol{R}_g)|\boldsymbol{r}_g|\phi_g(\boldsymbol{R}_g)\rangle, \quad (11)$$

$$\hbar\boldsymbol{K}_g=\langle\phi_g(\boldsymbol{R}_g)|\boldsymbol{p}_g|\phi_g(\boldsymbol{R}_g)\rangle. \quad (12)$$

In the case of $\boldsymbol{R}_1=\boldsymbol{R}_2=\boldsymbol{R}_g$, which corresponds to $\boldsymbol{R}=0$, the wave function describes the simplest case that two nucleons form the ideal pn cluster having the $(0s)^2$ configuration. The superposition of the $(0s)^2$ pn cluster wave functions with various $\boldsymbol{R}_g$ parameters is equivalent to the the generator coordinate method (GCM) of the two-body $^{16}\mathrm{O}+(pn)$ cluster model, in which $\boldsymbol{R}_g$ is treated as the generator coordinate describing the relative motion between the pn cluster and ^{16}O. Because of the Fermi statistics, the $(0s)^2$ pn cluster with the isospin $T=0$ is the pure spin-triplet ($S=1$) state, while that with $T=1$ is the spin-singlet ($S=0$) state. In the two-body $^{16}\mathrm{O}+(pn)$ cluster model, the $T=0$ and $T=1$ states of ^{18}F are composed of the $(TS)=(01)$ and (10) pn clusters, respectively.

In reality, the ideal $(0s)^2$ pn cluster is broken at the nuclear surface because of the effect from the core. Therefore, we extend the two-body $^{16}\mathrm{O}+(pn)$ cluster model to the three-body $^{16}\mathrm{O}+p+n$ model by taking into account $\boldsymbol{R}_1\neq\boldsymbol{R}_2$ cases and treat the parameter $\boldsymbol{R}=\boldsymbol{R}_1-\boldsymbol{R}_2$ as an additional generator coordinate to incorporate more general states of the pn pair having internal excitations. In the present calculation, we perform the GCM calculation of the three-body cluster model for ^{18}F by superposing the wave function $\Phi_{^{16}\mathrm{O}+pn}(\boldsymbol{R}_1,\boldsymbol{R}_2)$. Let us consider the body-fixed frame XYZ. We choose the $\boldsymbol{R}_g$ vector on the Z axis as $\boldsymbol{R}_g=(0,0,D_g)$ and the nucleon-spin (σ) orientation to the Y axis as spin-up ($\uparrow_Y$) or spin-down ($\downarrow_Y$) in the intrinsic wave function before projections. In the present GCM calculation for ^{18}F, we restrict the $\boldsymbol{R}$ vector on the XY plane and treat it as the generator coordinate as well as the coordinate D_g. Namely, the parameters chosen in the present GCM calculation are

$$\boldsymbol{R}=\left(\frac{i}{\nu}k_X,2d_Y,0\right), \quad (13)$$

$$\boldsymbol{R}_g=(0,0,D_g). \quad (14)$$

Here k_X, d_Y, and D_g are real parameters which are treated as the generator coordinates. Then the J^+ states of ^{18}F with $T=0$ and $T=1$ are given by the linear combination of the parity and total-angular-momentum eigenwave functions projected from $\Phi_{^{16}\mathrm{O}+pn}(\boldsymbol{R}_1,\boldsymbol{R}_2)$,

$$\Psi_{^{18}\mathrm{F}}(T,J^\pi)=\sum_{k_X,d_Y,D_g}c^{T,J^\pi}_{k_X,d_Y,D_g}P^{J\pi}_{MK}\Phi_{^{16}\mathrm{O}+pn}(\boldsymbol{R}_1,\boldsymbol{R}_2), \quad (15)$$

$$\Phi_{^{16}\mathrm{O}+pn}(\boldsymbol{R}_1,\boldsymbol{R}_2)=\mathcal{A}\{\Phi_{^{16}\mathrm{O}}\psi_{p\uparrow_Y}(\boldsymbol{R}_1)\psi_{n\downarrow_Y}(\boldsymbol{R}_2)\}, \quad (16)$$

$$\boldsymbol{R}_1=\left(i\frac{k_X}{2\nu},d_Y,D_g\right), \quad (17)$$

$$\boldsymbol{R}_2=\left(-i\frac{k_X}{2\nu},-d_Y,D_g\right). \quad (18)$$

Here $P^{J\pi}_{MK}$ is the parity and total-angular-momentum projection operator. Although each intrinsic wave function contains

both $T = 0$ and $T = 1$ components, the isospin symmetry is restored by the K projection, and $T = 0$ and $T = 1$ states are obtained by projecting onto odd and even K states, respectively. In the present work, $K = +1$ and $K = -1$ states are mixed for $T = 0$ states, and $K = 0$ is chosen for $T = 1$ states by ignoring the isospin breaking in the wave function. We omit high-K components to save the computational cost and avoid the numerical error in the total-angular-momentum projection. The coefficients $c^{T,J^\pi}_{k_X,d_Y,D_g}$ are determined by solving the Hill-Wheeler equation so as to minimize the energy of $\Psi_{^{18}\mathrm{F}}(T,J^\pi)$.

In the three-body cluster GCM calculation, choosing $\mathrm{Im}[R_X]$ as the generator coordinate is equivalent to choosing $\mathrm{Re}[R_X]$ as the generator coordinate. We here adopt the imaginary part $\mathrm{Im}[R_X] = k_X/\nu$ as the generator coordinate as given in Eqs. (17) and (18) because it is suitable to consider the $\uparrow_Y$ and $\downarrow_Y$ nucleons boosted by the spin-orbit potential at the nuclear surface to have finite momenta along the X direction. Thus, we take into account the degrees of R_X, R_Y but fix only $R_Z = 0$ to save the numerical cost. The c.m. motion of the pn pair is fully taken into account in the present calculation with the total-angular-momentum projection and the generator coordinate D_g.

To calculate the Gamow-Teller transition strengths from the ^{18}O to ^{18}F, we also perform the GCM calculation of ^{18}O by using the three-body $^{16}\mathrm{O} + n + n$ model in the same way,

$$\Psi_{^{18}\mathrm{O}}(T,J^\pi) = \sum_{k_X,d_Y,D_g} c^{T,J^\pi}_{k_X,d_Y,D_g} P^{J+}_{MK} \Phi_{^{16}\mathrm{O}+nn}(\boldsymbol{R}_1,\boldsymbol{R}_2), \tag{19}$$

$$\Phi_{^{16}\mathrm{O}+nn}(\boldsymbol{R}_1,\boldsymbol{R}_2) = \mathcal{A}\{\Phi_{^{16}\mathrm{O}}\psi_{n\uparrow_Y}(\boldsymbol{R}_1)\psi_{n\downarrow_Y}(\boldsymbol{R}_2)\}, \tag{20}$$

$$\boldsymbol{R}_1 = \left(i\frac{k_X}{2\nu}, d_Y, D_g\right), \tag{21}$$

$$\boldsymbol{R}_2 = \left(-i\frac{k_X}{2\nu}, -d_Y, D_g\right). \tag{22}$$

In a similar way to the $^{16}\mathrm{O} + p + n$ wave function, we also consider the $^{16}\mathrm{O} + 4N$ model to study the α cluster breaking at the surface of the ^{16}O core,

$$\Phi_{^{16}\mathrm{O}+4N}(\boldsymbol{R}_1,\boldsymbol{R}_2,\boldsymbol{R}_3,\boldsymbol{R}_4) = \mathcal{A}\{\Phi_{^{16}\mathrm{O}}\psi_{p\uparrow_Y}(\boldsymbol{R}_1)\psi_{p\downarrow_Y}(\boldsymbol{R}_2)\psi_{n\uparrow_Y}(\boldsymbol{R}_3)\psi_{n\downarrow_Y}(\boldsymbol{R}_4)\}. \tag{23}$$

III. RESULTS

A. Effective nuclear force

The present model is based on the microscopic A-body wave function with the assumption of the inert core. In the model, the Hamiltonian consists of the one-body kinetic term and the effective two-body nuclear forces and Coulomb force,

$$H = \sum_i t_i - T_G + \sum_{i<j} v^{\mathrm{eff}}_{ij} + \sum_{i<j} v^{\mathrm{Coul}}_{i,j}. \tag{24}$$

Here T_G is the kinetic energy of the total c.m. motion. We adopt the Volkov No. 2 force [30] for the effective central forces and supplement the spin-orbit force with the same form as the spin-orbit term of the G3RS force [31]. Then, the central and spin-orbit forces are expressed by two-range Gaussian forms,

$$v^{\mathrm{eff}}_{ij} = v_{\mathrm{c}}(r_{ij})\left[(1-m) + bP^\sigma_{ij} - hP^\tau_{ij} - mP^\sigma_{ij}P^\tau_{ij}\right] + v_{\mathrm{ls}}(r_{ij})P(^3\mathrm{O})(\boldsymbol{l}_{ij}\cdot\boldsymbol{S}_{ij}), \tag{25}$$

$$r_{ij} = |\boldsymbol{r}_i - \boldsymbol{r}_j|, \tag{26}$$

$$v_{\mathrm{c}}(r) = \sum_{k=1,2} v^c_k e^{-\frac{r^2}{a_k^2}}, \tag{27}$$

$$v_{\mathrm{ls}}(r_{ij}) = \sum_{k=1,2} v^{\mathrm{ls}}_k e^{-\frac{r^2}{a_k'^2}}, \tag{28}$$

where P^σ_{ij} and P^τ_{ij} are the spin and isospin exchange operators, $P(^3\mathrm{O})$ is the projection operator onto the triplet odd (^{3}O) state, $\boldsymbol{l}_{ij}$ is the angular momentum for the relative coordinate $\boldsymbol{r}_{ij} \equiv \boldsymbol{r}_i - \boldsymbol{r}_j$, and $\boldsymbol{S}_{ij}$ is the sum of the nucleon spins $\boldsymbol{S}_{ij} = \boldsymbol{s}_i + \boldsymbol{s}_j$. The constant values $v^c_{1,2}$ and $a_{1,2}$ are the strength and range parameters, respectively, of the central force given in the Volkov No. 2 force, and $v^{\mathrm{ls}}_{1,2}$ and $a'_{1,2}$ are those of the spin-orbit force in G3RS.

We choose the Majorana parameter $m = 0.62$, which is the same parameter used in Ref. [32], to reproduce the ^{20}Ne energy spectra measured from the threshold energy in the $^{16}\mathrm{O} + \alpha$ cluster model calculation. The b and h for Bartlett and Heisenberg terms are the adjustable parameters that change the relative strength of the nuclear forces in the ^{3}E and the ^{1}E channels. In the present calculation, we mainly use $b = h = 0.125$, which reproduces the deuteron binding energy in the ^{3}E channel as well as the unbound feature of two nucleons in the ^{1}E channel. The ratio f of the S-wave NN force in the ^{3}E channel to that in the ^{1}E channel is $f = (1+b+h)/(1-b-h) = 1.67$ for $b = h = 0.125$. Although those parameters describe reasonably the properties of two-nucleon systems in free space, they are found to overestimate excitation energies of the $T = 1$ states relative to the $T = 0$ states in ^{18}F. Therefore, we also demonstrate the results calculated with the parameter set $b = h = 0.06$ with the weaker ratio $f = 1.23$. We use the labels "bh125" and "bh06" for the interaction parameters $b = h = 0.125$ and $b = h = 0.06$, respectively.

For the strength of the two-body spin-orbit force, $v^{\mathrm{ls}}_1 = -v^{\mathrm{ls}}_2 \equiv u_{\mathrm{ls}} = 820$ MeV is chosen to reproduce the low-lying energy spectra of ^{17}O in the $^{16}\mathrm{O} + n$ model calculation (see Fig. 2). To discuss the effect of the spin-orbit force on the pn pair in ^{18}F, we perform calculations with and without the spin-orbit force.

For the two-body Coulomb force

$$v^{\mathrm{Coul}}_{i,j} = \sum_{i<j} \frac{1+P^\tau_i}{2}\frac{1+P^\tau_j}{2}\frac{e^2}{r_{ij}}, \tag{29}$$

the function $1/r$ is approximated by a sum of seven Gaussians.

B. Energy levels of ^{18}F

We perform the GCM calculation of the three-body $^{16}\mathrm{O} + p + n$ model. The generator coordinates, D_g, k_X, and d_Y are discretized as $D_g = 1,2,3,4,5$ fm, $k_X/2\nu = 0, 0.5, \ldots, a^{\max}_X$ fm with $a^{\max}_X = \min(1 + D_g, 2.5\ \mathrm{fm})$, and $d_Y = 0,1,2$ fm. We

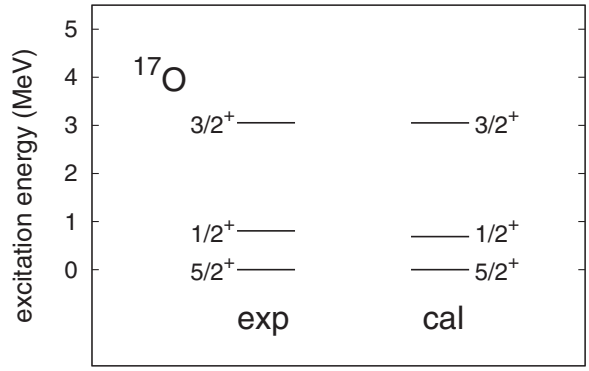

FIG. 2. Energy levels of ^{17}O. Theoretical energies are calculated by the GCM calculation of the two-body $^{16}\mathrm{O}+n$ model using the bh125 interaction with the spin-orbit force with the strength $u_{\mathrm{ls}} =$ 820 MeV.

check the convergence for the maximum values of these parameters, and it is found that, when basis wave functions with the maximum values are excluded, the change of the excitation energy is less than 0.1 MeV.

The calculated energy levels of ^{18}F are shown in Fig. 3 compared with the experimental data. In the result calculated with the spin-orbit force, we obtain $J^\pi = 1^+, 3^+, 5^+$ states, as well as the 2^+ state in the $T = 0$ channel and $J^\pi = 0^+$ and 2^+ states in the $T = 1$ channel. The calculated energy spectra in each $T = 0$ and $T = 1$ channel are in good agreement with the experimental data. However, in the result with the bh125 interaction, the relative energies of $T = 1$ states to the $T = 0$ states are overestimated compared with the experimental data. In the calculation with the bh06 interaction the experimental energy spectra of $T = 0$ and $T = 1$ states are reproduced reasonably. As mentioned before, the bh125 interaction is a reasonable effective nuclear force for two S-wave nucleons in free space. In the present three-body model for ^{18}F, we need to empirically modify the b and h parameters to reproduce the relative energy between $T = 0$ and $T = 1$ states. We do

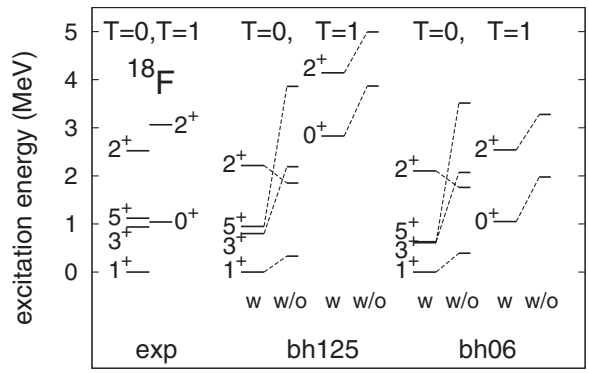

FIG. 3. Energy levels of $T = 0$, $J^\pi = 1^+$, 2^+, 3^+, and 5^+ states and $T = 1$, $J^\pi = 0^+$ and 2^+ states in ^{18}F obtained with the GCM calculation of the three-body $^{16}\mathrm{O}+p+n$ model in comparison with the experimental levels for the corresponding states. The results obtained with the bh125 and bh06 interactions are shown. The energies without the spin-orbit force measured from the $T = 0$, $J^\pi = 1^+$ energy obtained with the spin-orbit force are also shown.

not know the fundamental reason for the modification, but it may originate in the limitation of the effective two-body interaction in the microscopic calculation with the inert ^{16}O core assumption. It is found that structures of the ground and excited states do not depend so much on the choice of the bh125 and bh06 interactions except for the $T = 0$ and $T = 1$ relative energy. Therefore, in this paper, we mainly discuss the results calculated with the original bh125 interaction.

We also show the energy spectra calculated by switching off the spin-orbit force. The energies are measured from the $J^\pi = 1^+$ ground-state energy obtained with the spin-orbit force. In the energy spectra without the spin-orbit force, the intrinsic spin S decouples from the orbital-angular momentum L. As a result, the $T = 0$ levels can be understood by the simple $L = 0, 2$, and 4 spectra for $J = L \pm 1$ states in the LS coupling scheme. In the present calculation, slight coupling of L and S remains because of the truncation of the model space.

Comparing the spectra with and without the spin-orbit force, it is found that the $T = 0$ spectra are drastically changed by the spin-orbit force. The total energy gain due to the spin-orbit force is very small in the $J^\pi = 1^+$ state, while that in the 3^+ state is as large as about 1 MeV, and it is largest in the 5^+ state at about 3 MeV. Naively, the intrinsic spin $S = 1$ and the orbital angular momentum L of the $(TS) = (01)$ pn pair are parallel in the $J = L + 1$ states and two nucleons in the pn pair in high-spin states feel the attractive spin-orbit potential as understood by the rotation boost of the $T = 0$ pair while the pair in the $L = 0$ state feels no spin-orbit potential (see bottom panels of Fig. 1). This is the reason for the larger energy gain in higher spin states than lower spin states in the $T = 0$ energy spectra.

In the $T = 1$ energy spectra, the total energy gain due to the spin-orbit force is about 1 MeV in the $J^\pi = 0^+$ and 2^+ states. Compared with the drastic change in the $T = 0$ spectra, the 0^+-2^+ level spacing in the $T = 1$ spectra are not changed so much by the spin-orbit force. The spin-orbit potential energy gain of the $T = 1$ pn pair is caused by the opposite boost in the pair of the spin-up and -down nucleons (see top panels of Fig. 1).

Because of the larger energy gain with the spin-orbit force in the $T = 1$, $J^\pi = 0^+$ state than the $T = 0$, $J^\pi = 1^+$ state, the excitation energy of the $T = 1$, $J^\pi = 0^+$ state becomes lower than the case without the spin-orbit force. This result is consistent with the studies of the $T = 0$ pairing based on shell-model calculations and mean-field calculations in preceding works [5,12,15–18] that suggested the unlikely $T = 0$, $J^\pi = 1^+$ pair compared with the favored $T = 1$, $J^\pi = 0^+$ pair in the spin-orbit potential. It should be noted that in high-spin states the $T = 0$ pair is favored by the spin-orbit field. Detailed discussions of the energy gain mechanism of $T = 0$ and $T = 1$ pn pairs in the spin-orbit potential are given in the next section.

C. Spin components in ^{18}F

In ^{18}F, the $S = 1$ ($S = 0$) component mixes in the dominant $S = 0$ ($S = 1$) component in the $T = 1$ ($T = 0$) pair because of the spin-orbit force. Namely, the odd-parity mixing in the pn pair occurs. The mixed odd-parity component $\mathcal{P}_{\mathrm{odd}}$ in the pair can be measured by the expectation values of the squared

TABLE I. The expectation values $\langle \boldsymbol{S}^2 \rangle$ of the squared intrinsic spin of the $T = 0$ and $T = 1$ states of ^{18}F obtained by the GCM calculations of the three-body $^{16}\mathrm{O} + p + n$ model. The results calculated with the bh125 and the bh06 interactions with the spin-orbit force and the results of the bh125 force without the spin-orbit force are listed. The odd-parity component $\mathcal{P}_{\mathrm{odd}}$ in the pn pair for each state is also shown.

J^π, T	bh125		bh06		bh125 without ls	
	$\langle \boldsymbol{S}^2 \rangle$	$\mathcal{P}_{\mathrm{odd}}$	$\langle \boldsymbol{S}^2 \rangle$	$\mathcal{P}_{\mathrm{odd}}$	$\langle \boldsymbol{S}^2 \rangle$	$\mathcal{P}_{\mathrm{odd}}$
$0^+, T = 1$	0.23	0.11	0.19	0.09	0.00	0.00
$2^+, T = 1$	0.27	0.14	0.21	0.11	0.00	0.00
$1^+, T = 0$	1.91	0.05	1.89	0.06	2.00	0.00
$3^+, T = 0$	1.95	0.02	1.94	0.03	2.00	0.00
$5^+, T = 0$	2.00	0.00	2.00	0.00	2.00	0.00
$2^+, T = 0$	1.95	0.03	1.93	0.04	2.00	0.00

intrinsic spin $\langle \boldsymbol{S} \rangle^2$ as $\mathcal{P}_{\mathrm{odd}} = 1 - \langle \boldsymbol{S}^2 \rangle/2$ for the $T = 0$ states and $\mathcal{P}_{\mathrm{odd}} = \langle \boldsymbol{S}^2 \rangle/2$ for the $T = 1$ states.

The calculated values of $\langle \boldsymbol{S}^2 \rangle$ and $\mathcal{P}_{\mathrm{odd}}$ for the ^{18}F states obtained by the GCM calculation are shown in Table I. In the results obtained with the spin-orbit force, the odd-parity mixing is found to be larger in the $T = 1$ states than in the $T = 0$ states. In other words, the parity mixing occurs in the $T = 1$ pair, while the parity mixing is suppressed in the $T = 0$ pair. It is simply understood by the roles of the spin-orbit potential that cause the opposite boost in the $T = 1$ pair with the parity mixing and the rotation boost of the $T = 0$ pair with no internal structure change.

D. $M1$ and GT Transitions of ^{18}F

To check the reliability of spin configurations in the present calculation, we show the calculated values of the magnetic moments, the $M1$ transition strength, and the GT transition strength of ^{18}F and compare them with the experimental data in Table II. For $B(\mathrm{GT})$, we perform the GCM calculation of the $^{16}\mathrm{O} + n + n$ model to obtain the ^{18}O ground state in the same way as that in the $^{16}\mathrm{O} + p + n$ model for ^{18}F. The calculated results are in reasonable agreement with the experimental data.

As discussed before, the dominant components of the $T = 0$, $J^\pi = 1^+$, 3^+, and 5^+ states are the $S = 1$ states coupling with the orbital angular momentum $L = 0$, 2, and 4, and the mixing of the $S = 0$ component is minor. Therefore, the magnetic moments of these states are not sensitive to the interaction because the intrinsic spin configurations do not depend so much on the interaction.

TABLE II. The magnetic moments of $^{18}\mathrm{F}(1^+)$, $^{18}\mathrm{F}(3^+)$, and $^{18}\mathrm{F}(5^+)$, the $B(M1)$ for the transition $^{18}\mathrm{F}(0^+) \to {}^{18}\mathrm{F}(1^+)$, and the $B(\mathrm{GT})$ for the transition $^{18}\mathrm{O}(0^+) \to {}^{18}\mathrm{F}(1^+)$. The results calculated with the bh125 and bh06 interactions with the spin-orbit force, and the bh125 interaction without the spin-orbit force are shown. The experimental data are taken from Refs. [33,34].

	Exp.	bh125	bh06	w/o ls
$\mu(1^+)$ (μ_N)	–	0.82	0.82	0.82
$\mu(3^+)$ (μ_N)	1.77(12)	1.86	1.85	1.84
$\mu(5^+)$ (μ_N)	2.86(3)	2.88	2.88	2.88
$B(M1; 0^+)$ (μ_N^2)	19.5(3.8)	17.0	17.4	14.1
$B(\mathrm{GT})$ $\left(g_A^2/4\pi\right)$	3.18	5.0	5.2	10.7

The results of $B(M1)$ for $^{18}\mathrm{F}(0^+) \to {}^{18}\mathrm{F}(1^+)$ and $B(\mathrm{GT})$ for $^{18}\mathrm{O}(0^+) \to {}^{18}\mathrm{F}(1^+)$ obtained using the bh125 interactions with the spin-orbit force are similar to those using the bh06 interaction with the spin-orbit force. However, they are somewhat different from the result obtained without the spin-orbit force because the spin structure changes significantly in the $T = 1$, $J^\pi = 0^+$ state reflecting the $S = 1$ mixing, i.e., the parity mixing in the $T = 1$ pair. In the result without the spin-orbit force, $B(\mathrm{GT})$ is remarkably large, showing that the transition is the superallowed transition given by the spin-isospin flip from the $S = 1$ pn pair in $^{18}\mathrm{F}(1^+)$ to the $S = 0$ nn pair in $^{18}\mathrm{O}(0^+)$. With the spin-orbit force, $B(\mathrm{GT})$ becomes small because the spin structure of the nn pair in $^{18}\mathrm{O}(0^+)$ is changed by the spin-orbit force.

IV. DISCUSSION

We discuss here the effect of the spin-orbit potential on the pn pair at the nuclear surface, in particular, the effect on the internal structure of the pair and that on the c.m. motion of the pair. We show that the symmetry breaking, i.e., the odd-parity mixing in the pair occurs due to the spin-orbit field from the core nucleus.

A. Basic idea of effect of spin-orbit field on a pn pair at nuclear surface

As shown before, the ^{18}F energy spectra obtained without the spin-orbit force can be understood by the dinucleon picture for $(TS) = (10)$ and $(TS) = (01)$ pairs moving in L waves around the ^{16}O core. In the case with the spin-orbit force, $T = 1$ states are favored by the spin-orbit field involving the odd-parity mixing in the pair, while the $T = 0$ pair in high-L states is favored largely without the odd-parity mixing in the pair. These are consistent with the naive expectation from the opposite boost in the $T = 1$ pair and the rotation boost of the $T = 0$ pair by the spin-orbit force.

To understand features of the pn pair around the ^{16}O core in more detail, we consider a single wave function $\Phi_{^{16}\mathrm{O}+pn}(\boldsymbol{R}_1, \boldsymbol{R}_1)$ which expresses a pn pair localized around a certain position $\boldsymbol{R}_g$ at the surface of the core in the body-fixed XYZ frame defined in Sec. II. Starting from the ideal dinucleon of the $(0s)^2$ pn pair in the case without the spin-orbit field and considering the spin-orbit force as the perturbative external field from the core, we discuss how the pair behavior is affected by the spin-orbit field. The ideal $(0s)^2$ pn pair localized around the position $(0,0,D_g)$ is written by $\Phi_{^{16}\mathrm{O}+pn}(\boldsymbol{R}_1, \boldsymbol{R}_2)$ with $\boldsymbol{R}_1 = \boldsymbol{R}_2 = (0,0,D_g)$. We consider the parallel-spin pair as consisting of a $\uparrow_Y$ proton and a $\uparrow_Y$ neutron and the antiparallel-spin pair as consisting of a $\uparrow_Y$ proton and a $\downarrow_Y$ neutron in the intrinsic frame XYZ. The former is the $(TS) = (01)$ state, and the latter contains the $T = 0$ and $T = 1$ components. In the following, we first discuss the pair behavior in the intrinsic frame, and later we discuss it in the laboratory

frame and consider the decomposition of the $\uparrow_Y\downarrow_Y$ pair into $T = 1$ and $T = 0$ components by the $J_Z = K$ projection.

When the spin-orbit force is switched on, the one-body spin-orbit field from the ^{16}O core causes the rotation boost of the $\uparrow_Y\uparrow_Y$ pair and the opposite boost in the $\uparrow_Y\downarrow_Y$ pair as shown in Fig. 1. The boost mechanism by the spin-orbit potential can be understood by the following classical picture of the Gaussian wave packet for each nucleon moving on the XY plane passing through the $(0,0,D_g)$. The nucleon at the position $(0,0,D_g)$ having the finite momentum $\boldsymbol{k}_i = (k_{jX},k_{jY},0)$ has the angular momentum $\boldsymbol{l}_i = D_g(-k_{jY},k_{jX},0)$. Assuming the averaged one-body spin-orbit potential around the position $(0,0,D_g)$ as $-\bar{U}_{ls}\boldsymbol{l}_i\cdot\boldsymbol{s}_i$ with a constant positive value $\bar{U}_{ls}$, the spin-orbit potential energy gain is given as $-\frac{\bar{U}_{ls}D_g}{2}k_{jX}$ for the $\uparrow_Y$ nucleon and $\frac{\bar{U}_{ls}D_g}{2}k_{jX}$ for the $\downarrow_Y$ nucleon. It means that the spin-orbit potential energy gain is proportional to the nucleon momentum k_{jX} and it makes k_{jX} of the $\uparrow_Y(\downarrow_Y)$ nucleon to be positive(negative) and causes the rotation boost for the $\uparrow_Y\uparrow_Y$ pair and the opposite boost for the $\downarrow_Y\uparrow_Y$ pair.

As for the $\uparrow_Y\uparrow_Y$ pair for the $T = 0$ pair, the ideal case for the rotation boost is described by taking the parameter set $\boldsymbol{R}_1 = \boldsymbol{R}_2 = (i\kappa_X/2\nu,0,D_g)$ in the $\Phi_{^{16}\mathrm{O}+pn}(\boldsymbol{R}_1,\boldsymbol{R}_2)$ model wave function. (Here we define the nucleon momenta $\kappa_X = k_{1X} = k_{2X}$ for the $\uparrow_Y\uparrow_Y$ pair.) The internal pair wave function $\phi_{\mathrm{in}}(\boldsymbol{R};\boldsymbol{r})$ in Eq. (6) for the case $\boldsymbol{R} = \boldsymbol{R}_1 - \boldsymbol{R}_2 = 0$ is consistent with the $(0s)^2$ pn pair, while the c.m. wave function of the pair $\phi_g(\boldsymbol{R}_g;\boldsymbol{r}_g)$ in Eq. (5) for the case $\boldsymbol{R}_g = (i\kappa_X/2\nu,0,D_g)$ indicates the pn pair localized around the position $\boldsymbol{D}_g = (0,0,D_g)$ with the finite momentum $\boldsymbol{K}_g = (2\kappa_X,0,0)$. It means that the rotation boost of the pair occurs keeping the internal pair wave function unchanged.

However, for the $\uparrow_Y\downarrow_Y$ pair the spin-orbit potential causes the opposite boost in the pair with the P-wave mixing to the dominant S-wave component in the internal wave function of the pair. In the $\Phi_{^{16}\mathrm{O}+pn}(\boldsymbol{R}_1,\boldsymbol{R}_2)$ model wave function, the odd-parity mixing is clearly described by the nucleon momentum, which is interpreted as the order parameter of the symmetry breaking as follows. The ideal case of the opposite boost is described by taking the parameter set $\boldsymbol{R}_1 = (ik_X/2\nu,0,D_g)$ and $\boldsymbol{R}_2 = (-ik_X/2\nu,0,D_g)$ in the $\Phi_{^{16}\mathrm{O}+pn}(\boldsymbol{R}_1,\boldsymbol{R}_2)$ model. The $\uparrow_Y\downarrow_Y$ pair with the opposite nucleon momenta k_X is no longer the $(0s)^2$ pair, but it contains the odd-parity mixing in the dominant even-parity component as shown in the internal pair wave function $\phi_{\mathrm{in}}(\boldsymbol{R};\mathbf{r})$ of Eq. (6) for the case $\boldsymbol{R} = \boldsymbol{R}_1 - \boldsymbol{R}_2 = (ik_X/\nu,0,0)$,

$$\phi_{\mathrm{in}}(\boldsymbol{R};\boldsymbol{r}) = \left(\frac{\nu}{\pi}\right)^{3/4} e^{-\frac{\nu}{2}(x-ik_X/\nu)^2-\frac{\nu}{2}y^2-\frac{\nu}{2}z^2}, \tag{30}$$

and more explicitly in the Taylor expansion with respect to k_X,

$$\begin{aligned}\phi_{\mathrm{in}}(\boldsymbol{R};\boldsymbol{r}) &\propto \left(\frac{\nu}{\pi}\right)^{3/4}\left[1 + ik_X x + \mathcal{O}\left(k_X^2\right)\right]e^{-\frac{\nu}{2}\boldsymbol{r}^2} \\ &= (0,0,0)_{\mathrm{ho}} + i\sqrt{\frac{1}{2\nu}}k_X(1,0,0)_{\mathrm{ho}} + \mathcal{O}\left(k_X^2\right). \end{aligned}\tag{31}$$

Here $(n_X,n_Y,n_Z)_{\mathrm{ho}}$ is the H.O. solution for the width $b^2 = 1/\nu$. The square of the coefficient $k_X^2/2\nu$ of the second term is estimated as $k_X^2/2\nu \leqslant 0.125$ for the typical value $k_X \leqslant 0.2$ fm^{-1} optimized for the pn pair in the intrinsic frame of the $^{16}\mathrm{O} + pn$ system, as shown later. Therefore, the second term is minor compared with the leading term (the first term). This means the minor mixing of the P-wave $(1,0,0)_{\mathrm{ho}}$ component in the dominant S-wave $(0,0,0)_{\mathrm{ho}}$ state. Namely, the parity mixing, i.e., the symmetry breaking in the $\uparrow_Y\downarrow_Y$ pair occurs because of the external spin-orbit field. Here the parameter k_X is regarded as the order parameter for the symmetry breaking. The energy gain is the second-order perturbation caused by the transition from the S-wave state to the P-wave state. The spin-orbit potential energy gain of the $\uparrow_Y\downarrow_Y$ pair is proportional to k_X and it is mainly given by the nondiagonal matrix elements of the spin-orbit potential between the S-wave and P-wave states in the pair. Because the odd-parity mixing inevitably causes the internal energy loss of the pair, the mixing ratio of the odd-parity component to the even-parity component in the $\uparrow_Y\downarrow_Y$ pair is determined by the competition between the spin-orbit potential energy gain and the internal energy loss. The parity-mixing mechanism in the dinucleon pair is also explained in Appendix A.

We consider the correspondence of the pn pair around the ^{16}O core in the intrinsic frame to the ^{18}F states in the laboratory frame where the rotational symmetries in the total system are restored by the parity and total-angular-momentum projections. For the $\uparrow_Y\uparrow_Y$ pair, the spin-orbit field causes the rotational excitation of the c.m. motion of the pair in the body-fixed frame. It means that, in the laboratory frame, the $(TS) = (01)$ pair in high L states is favored by the spin-orbit field. This is a naive explanation for the larger energy gain of the spin-orbit in the higher spin states in the $T = 0$ spectra of ^{18}F in the GCM calculation shown in Fig. 3. However, for the $\uparrow_Y\downarrow_Y$ pair, the spin-orbit potential changes the internal structure of the pair involving the odd-parity mixing while the c.m. motion of the pair in the body-fixed frame is not affected by the spin-orbit force. In the laboratory frame, it leads to less sensitivity of the the 0^+-2^+ level spacing in the $T = 1$ spectra of ^{18}F on the spin-orbit force in the GCM calculation.

The $\uparrow_Y\downarrow_Y$ pair localized around $(0,0,D_g)$ contains the $T = 1$ and $T = 0$ components, which are decomposed by the $J_Z = K$ projection. In the case of the high-spin $J^\pi = 3^+$ and 5^+ states, the $\uparrow_Y\uparrow_Y$ pair moving in $L = 2$ and $L = 4$ wave is naively expected to be favored because it gains the spin-orbit potential energy without the internal energy loss. For the $J^\pi = 1^+$ state, we can consider the $T = 0$ component projected from the $\uparrow_Y\downarrow_Y$ pair instead of the $\uparrow_Y\uparrow_Y$ pair because there is no energy gain for the $\uparrow_Y\uparrow_Y$ pair in the $L = 0$ wave. However, in the $T = 0$ component of the $\uparrow_Y\downarrow_Y$ pair, the odd-parity mixing in the pair is unfavored because it suffers from the larger internal energy loss compared with the $T = 1$ component of the $\uparrow_Y\downarrow_Y$ pair because of the following reason. The $T = 1$ and $T = 0$ components of the $\uparrow_Y\downarrow_Y$ pair are obtained by the $K = 0$ and $K = 1$ projections, respectively. For a given finite value of k_X, the odd-parity mixing becomes half of the intrinsic state in the $K = 0$ projected state for the $T = 1$ component but it is not the case in the $K = 1$ state for the $T = 0$ component as explained in Appendix A. As a result of the less internal energy loss in the $T = 1$ pair than the $T = 0$ pair, the $T = 1$ pair efficiently gains the spin-orbit potential involving the parity

mixing. In other words, the total energy gain of the $\uparrow_Y\downarrow_Y$ pair with the odd-parity mixing in the spin-orbit potential is not so efficient for the $T = 0$ pair in the $J^\pi = 1^+$ state as the $T = 1$ pair in the $J^\pi = 0^+$ state. More quantitative discussion is given in the later analysis.

This mechanism of the unfavorable $T = 0$, $J^\pi = 1^\pi$ pair in the spin-orbit potential is consistent with that argued by Bertsch [18]. It is also consistent with the discussions in Refs. [5,12,15–17], where the relation between the jj coupling and the LS coupling schemes was discussed. One of the new standpoints in the present dinucleon picture is that we focus on the internal pair wave function and discuss its change involving the odd-parity mixing because of the spin-orbit force. That is to say, starting from the $S = 0$ pair with the pure even-parity component in the case without the spin-orbit field, we consider the odd-parity ($S = 1$) mixing in the pair caused by the perturbative spin-orbit field. This is an alternative interpretation of the mean-field picture in the jj coupling scheme where even-parity ($S = 0$) and odd-parity ($S = 1$) components are already mixed in the j^2 state in no correlation limit and the enhancement of the even-parity component by the pair correlation is taken into account.

Generally, in J^π states after the parity and total-angular-momentum projections, internal degrees of freedom in the pair and the c.m. motion of the pair are not separable. Note that the odd-parity component in the pair couples with the odd-parity wave of the pair c.m. motion around the core in the J^+ states in the laboratory frame. Moreover, because of the effect of the antisymmetrization from the core, the single-particle wave functions of nucleons in the pair are not localized Gaussian wave packets in the total system, and the internal pair wave function is not the pure S-wave state even in the $k_X = 0$ case when we take into account the orthogonality to the occupied orbits as explained in Appendix B. Strictly speaking, it is not able to define the internal wave function separately from the c.m. motion because of the projections and the antisymmetrization, and the partial-wave expansion of the internal wave function in Eq. (31) is not valid any more. Nevertheless, because the Hamiltonian for two nucleons around the ^{16}O core is still invariant for the rotation around the Z axis, it is able to consider the symmetry breaking, i.e., the odd-parity mixing in the antiparallel-spin pair by the spin-orbit field in a way similar to the present idea as explained in Appendix A, and we can measure the mixing of the odd-parity components by the spin-singlet and spin-triplet components in the physical $T = 0$ and $T = 1$ states of ^{18}F, respectively, according to Fermi statistics of nucleons. Although the relation between the parameter k_X and the odd-parity component $\mathcal{P}_{\rm odd}$ in the $\Phi_{^{16}{\rm O}+pn}(\boldsymbol{R}_1,\boldsymbol{R}_2)$ model wave function is not as simple as the one derived from Eq. (31) after the antisymmetrization and the projections, k_X and $\mathcal{P}_{\rm odd}$ have the one-to-one correspondence for J^π-projected states for each spin and parity, as shown later. It means that the odd-parity mixing in the pair can be defined and has the physical meaning even in ^{18}F states in the laboratory frame, and k_X in $\Phi_{^{16}{\rm O}+pn}(\boldsymbol{R}_1,\boldsymbol{R}_2)$ can be regarded as an order parameter of the parity mixing.

It should be commented that the dinucleon cluster in ^{18}F has a large spatial overlap with the ^{16}O and the single-particle wave functions of two nucleons in the dinucleon are dominated by $(sd)^2$ configurations. In such a case, the parameter D_g in $\Phi_{^{16}{\rm O}+pn}(\boldsymbol{R}_1,\boldsymbol{R}_2)$ does not necessarily mean the distance of the pair from the ^{16}O core, though it relates to the spatial development of the pn pair from the core which can be expressed by the mixing of higher configurations beyond the sd shell. Even though the one-center basis representation in terms of shell-model configurations is useful to discuss single-particle motion, it is not suitable to discuss the internal wave function of the pair. In the analysis below, we discuss the pn pair behavior based on the dinucleon picture because this picture is useful to discuss the internal structure of the pn pair and helpful to understand the pn pair correlation at the surface of the ^{16}O core. The parameters D_g and k_X in the $\Phi_{^{16}{\rm O}+pn}(\boldsymbol{R}_1,\boldsymbol{R}_2)$ model wave function are indicators for the degree of the spatial development of the pair from the core and that of the odd-parity mixing in the pair, respectively.

B. Analysis based on a single ^{16}O + pn cluster wave function

As mentioned, the spin-orbit force changes the internal structure of the $\uparrow_Y\downarrow_Y$ pair and the c.m. motion of the $\uparrow_Y\uparrow_Y$ pair in the body-fixed frame. We here demonstrate how the parity mixing of the $T = 1$ pair occurs in the microscopic ^{18}F system based on two-body effective nuclear forces. We analyze the energy expectation value of a single three-body $^{16}{\rm O} + p + n$ wave function $\Phi_{^{16}{\rm O}+pn}(\boldsymbol{R}_1,\boldsymbol{R}_2)$ and quantitatively discuss the effect of the spin-orbit force on the $T = 1$ and the $T = 0$ pairs.

In the wave function $\Phi_{^{16}{\rm O}+pn}(\boldsymbol{R}_1,\boldsymbol{R}_2)$, single-nucleon wave functions for two nucleons in the pn pair are specified by the complex parameters $\boldsymbol{R}_1$ and $\boldsymbol{R}_2$, which express the centers of single-nucleon Gaussian wave packets in the phase space. To see the behavior of the pn pair localized around a certain position $\boldsymbol{R}_g = (\boldsymbol{R}_1 + \boldsymbol{R}_2)/2 = (0,0,D_g)$ with the distance D_g from the core, we vary the parameters $\boldsymbol{R}_1$ and $\boldsymbol{R}_2$ on the XY plane passing through the $(0,0,D_g)$ and obtain the energy minimum solution under the constraints $R_{1X} = -R_{2X}$, $R_{1Y} = -R_{2Y}$, and $R_{1Z} = R_{1Z} = D_g$.

We first perform the energy variation with respect to the intrinsic state $\Phi_{^{16}{\rm O}+pn}(\boldsymbol{R}_1,\boldsymbol{R}_2)$ without the parity and the total-angular-momentum projections,

$$\delta\frac{\langle\Phi_{^{16}{\rm O}+pn}(\boldsymbol{R}_1,\boldsymbol{R}_2)|H|\Phi_{^{16}{\rm O}+pn}(\boldsymbol{R}_1,\boldsymbol{R}_2)\rangle}{\langle\Phi_{^{16}{\rm O}+pn}(\boldsymbol{R}_1,\boldsymbol{R}_2)|\Phi_{^{16}{\rm O}+pn}(\boldsymbol{R}_1,\boldsymbol{R}_2)\rangle} = 0. \qquad (32)$$

The $\uparrow_Y\downarrow_Y$ and $\uparrow_Y\uparrow_Y$ pairs are considered. The former contains the $T = 0$ and $T = 1$ components, while the latter is regarded as the $T = 0$ pair. In the total-angular-momentum projection, the isospin symmetry is restored in the K projection.

After the variation, the energy minimum state in the intrinsic system is obtained. In the result of the $\uparrow_Y\downarrow_Y$ pair without the spin-orbit force, the optimized parameters for the energy minimum solution are $\boldsymbol{R}_1 \approx \boldsymbol{R}_2 \approx (0,0,D_g)$, indicating that the $(0s)^2$ pn pair is formed in the intrinsic system. When the spin-orbit force is switched on, the optimized $\boldsymbol{R}_j$ has the finite imaginary part as $\boldsymbol{R}_1 \approx (ik_X/2\nu,0,D_g)$ and $\boldsymbol{R}_2 \approx (-ik_X/2\nu,0,D_g)$, indicating the opposite boost in the pn

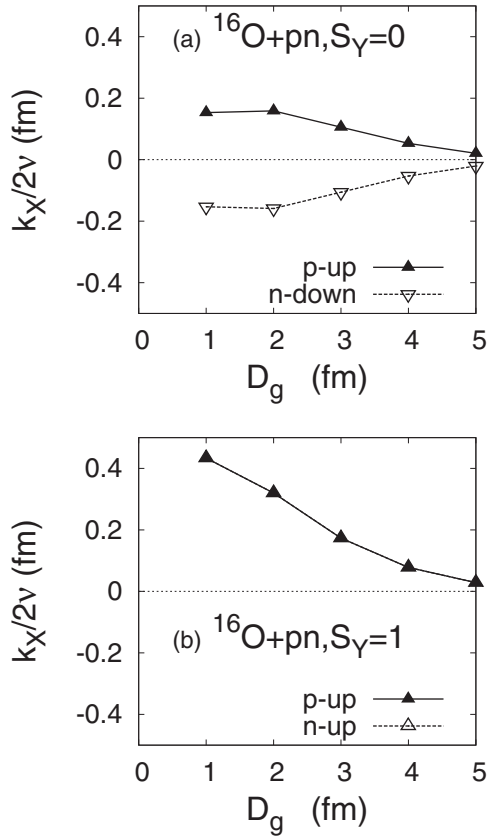

FIG. 4. The D_g dependence of k_{jX} obtained by the energy variation for the intrinsic wave function $\Phi_{^{16}\mathrm{O}+pn}(\boldsymbol{R}_1,\boldsymbol{R}_2)$ without the parity and total-angular-momentum projections. (Top) k_{jX} for the $\uparrow_Y\downarrow_Y$ pn pair. (Bottom) k_{jX} for the $\uparrow_Y\uparrow_Y$ pn pair. In the bottom panel, two lines for protons and neutrons overlap with each other because $k_{1X} \approx k_{2X}$. The bh125 interaction with the spin-orbit force is used.

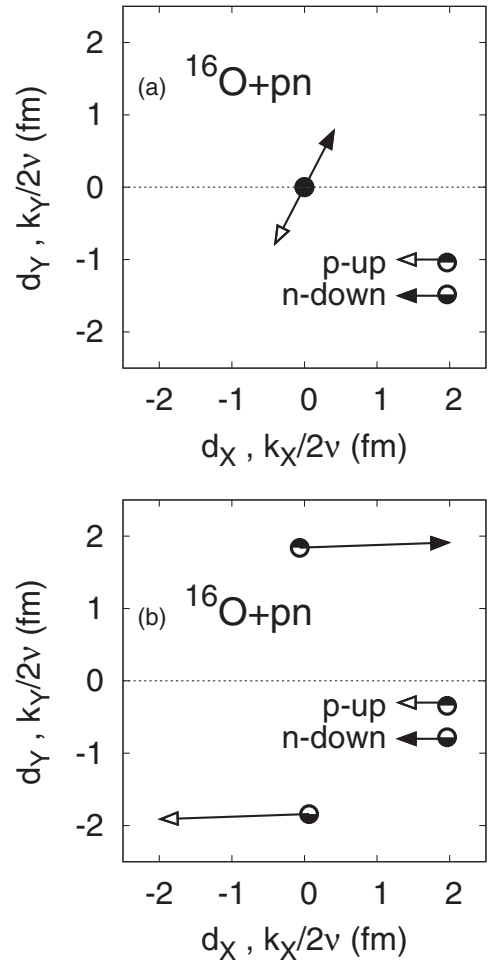

FIG. 5. $\boldsymbol{R}_1$ and $\boldsymbol{R}_2$ in $\Phi_{^{16}\mathrm{O}+pn}(\boldsymbol{R}_1,\boldsymbol{R}_2)$ for the $\uparrow_Y\downarrow_Y$ pn pair around $D_g = 2$ fm obtained by the VAP calculation for (a) the $T = 1$, $J^\pi = 0^+$ state and (b) the $T = 0$, $J^\pi = 1^+$ state. The real parts (d_{jX},d_{jY}) are shown as the positions on the XY plane, and the imaginary parts $(k_{jX}/2\nu,k_{jY}/2\nu)$ are illustrated by the lengths of the arrows. The bh125 interaction with the spin-orbit force is used.

pair around $(0,0,D_g)$ of $\uparrow_Y$ and $\downarrow_Y$ nucleons having the finite momentum k_X. The k_X for the nucleon momentum in the X direction is regarded as the order parameter as explained before, and the finite momentum k_X means that the parity symmetry in the pair is broken because of the external spin-orbit field. In Fig. 4(a), we show the D_g dependence of the nucleon momentum k_{jX} in the $\uparrow_Y\downarrow_Y$ pn pair. $k_X = k_{1X} = -k_{2X}$ is the largest at the distance $D_g = 2$ fm from the core and it gradually decreases as D_g increases because the spin-orbit potential from the core gets weak with the increase of D_g.

For the $\uparrow_Y\uparrow_Y$ pair, we take off the constraint $\mathrm{Im}[R_{gX}] = 0$ and perform the energy variation with the constraints $\mathrm{Re}[R_{1X}] = -\mathrm{Re}[R_{2X}]$, $R_{1Y} = -R_{2Y}$, and $R_{1Z} = R_{1Z} = D_g$ because two nucleons cannot be boosted in the same direction under the constraint of $\mathrm{Im}[R_{gX}] = 0$. As expected from the role of the spin-orbit field boosting nucleons at the surface, we obtain the minimum energy solution with $\boldsymbol{R}_1 \approx \boldsymbol{R}_2 \approx (i\kappa_X/2\nu,0,D_g)$, indicating two nucleons boosted in the same direction corresponding to the rotation boost of the $(0s)^2$ pn pair with the finite momentum $K_{gX} = 2\kappa_X$. The D_g dependence of the optimized k_{jX} for the $\uparrow_Y\uparrow_Y$ pair is shown in Fig. 4(b). $\kappa_X = k_{1X} = k_{2X}$ decreases as D_g increases.

We also perform the energy variation for the parity and total-angular-momentum projected states,

$$\delta\frac{\langle\Psi|H|\Psi\rangle}{\langle\Psi|\Psi\rangle} = 0, \tag{33}$$

$$\Psi = P^{J+}_{MK}\Phi_{^{16}\mathrm{O}+pn}(\boldsymbol{R}_1,\boldsymbol{R}_2). \tag{34}$$

Here $K = 0$ and $K = 1$ are chosen for $T = 1$ and $T = 0$ states, respectively. This is the variation after the projection (VAP). After the variation, the optimized parameters $\boldsymbol{R}_1$ and $\boldsymbol{R}_2$ of the energy minimum state for the J^π state are obtained. The VAP is performed for the $\uparrow_Y\downarrow_Y$ pair under the constraints $R_{1X} = -R_{2X}$, $R_{1Y} = -R_{2Y}$, and $R_{1Z} = R_{2Z} = D_g$. D_g is fixed to be 2 fm. The obtained results of $\boldsymbol{R}_j = \boldsymbol{d}_j + i\boldsymbol{k}_j/2\nu$ for the $T = 1$, $J^\pi = 0^+$ state and those for the $T = 0$, $J^\pi = 1^+$ state are shown in Fig. 5. The position $\boldsymbol{d}_j$ and the momentum $\boldsymbol{k}_j$ are projected onto the XY plane. Similarly to the variation without the projection, the k_{jX} values obtained in the VAP for the 1^+ and 0^+ states are finite and they are opposite for two

nucleons in the $\uparrow_Y\downarrow_Y$ pair so as to gain the spin-orbit potential. It is consistent with the simple picture of the opposite boost in the $\uparrow_Y\downarrow_Y$ pair. In addition, the 1^+ and 0^+ states obtained in the VAP have the finite d_{jY} and k_{jY} values, respectively. It indicates that the internal structure of the pair in the J^π states somewhat changes from the ideal $(0s)^2$ configuration because of core effects such as the central potential and also the antisymmetrization effects as well as the spin-orbit potential. This means that the GCM calculation with only one generator coordinate of R_X is not sufficient but that with two generator coordinates of R_X and R_Y is effective. Note that finite d_{jY} and k_{jY} are obtained only in the VAP but not in the variation without the projections in which the axial symmetry tends to be favored. The finite d_{jY} in the $T = 0$, $J^\pi = 1^+$ state may indicate that the size of the $T = 0$ pn pair is not so compact as that of the $(0s)^2$ cluster.

In spite of the finite $\boldsymbol{R}_{jY}$ for the $\uparrow_Y\downarrow_Y$ pair, the momentum $k_X = k_{1X} = -k_{2X}$ in the X direction is regarded as the order parameter for the symmetry breaking caused by the spin-orbit field from the core. To clarify the role of the spin-orbit force in the pn pair, we perform further analysis of the k_X dependence of the total energy of $\Phi_{^{16}\mathrm{O}+pn}(\boldsymbol{R}_1,\boldsymbol{R}_2)$ with fixed parameters $R_{jY} = 0$ and $R_{jZ} = D_g$. In the following, we choose $D_g =$ 2 fm for the center position of the pair.

We show in Figs. 6(a)–6(c) the energy of $\Phi_{^{16}\mathrm{O}+pn}(\boldsymbol{R}_1,\boldsymbol{R}_2)$ for the $\uparrow_Y\downarrow_Y$ pn pair with the parameters $\boldsymbol{R}_1 = (ik_X/2\nu,0,D_g)$ and $\boldsymbol{R}_2 = (-ik_X/2\nu,0,D_g)$ ($D_g = 2$ fm) as functions of k_X. It corresponds to the opposite boost in the pair (see the top panels of Fig. 1). The intrinsic wave function $\Phi_{^{16}\mathrm{O}+pn}(\boldsymbol{R}_1,\boldsymbol{R}_2)$ for the $\uparrow_Y\downarrow_Y$ pair contains the $T = 1$ and $T = 0$ components which are decomposed by the $K = 0$ and $K = 1$ projections. Energies for the intrinsic (no-projected) state are shown in Fig. 6(a), and those for the J^π-projected states are shown in Figs. 6(b) and 6(c). The J^π-projected energy is calculated by $P^{J^\pi}_{MK}\Phi_{^{16}\mathrm{O}+pn}(\boldsymbol{R}_1,\boldsymbol{R}_2)$ with $K = 0$ for the $J^\pi = 0^+$ and 2^+ states in the $T = 1$ channel and $K = 1$ for the $J^\pi = 1^+$ and 3^+ states in the $T = 0$ channel.

In the case without the spin-orbit force, the energy is minimum at $k_X = 0$ corresponding to no symmetry breaking, i.e., no parity mixing in the pair for the intrinsic state and all J^π projected states for the $\uparrow_Y\downarrow_Y$ pair. In the case with the spin-orbit force, the energy minimum of the intrinsic state shifts to the finite k_X region, indicating that the symmetry is broken by the spin-orbit potential. The total energy gain due to the spin-orbit force, which is estimated by the difference between the energy minima for the results with and without the spin-orbit force, is found to be large in the $T = 1$, $J^\pi = 0^+$ and 2^+ projected states [see Fig. 6(b)]. In particular, the $T = 1$, $J^\pi = 0^+$ state largely gains the energy due to the spin-orbit force. The energy curve without the spin-orbit force is more soft against the finite k_X in the $T = 1$, $J^\pi = 0^+$ and 2^+ states [Fig. 6(b)] than in the $T = 0$ states [Fig. 6(c)], indicating that the internal energy loss in the $T = 1$ pair with the finite k_X is milder than in the $T = 0$ pair. For the $T = 1$, $J^\pi = 0^+$ and 2^+ states [Fig. 6(b)], there is no spin-orbit potential contribution at the $k_X = 0$ for the pure $(TS) = (10)$ state with which the expectation value of the spin-orbit potential vanishes, but the spin-orbit potential energy efficiently contributes to the total energy gain in the finite k_X region involving the parity mixing

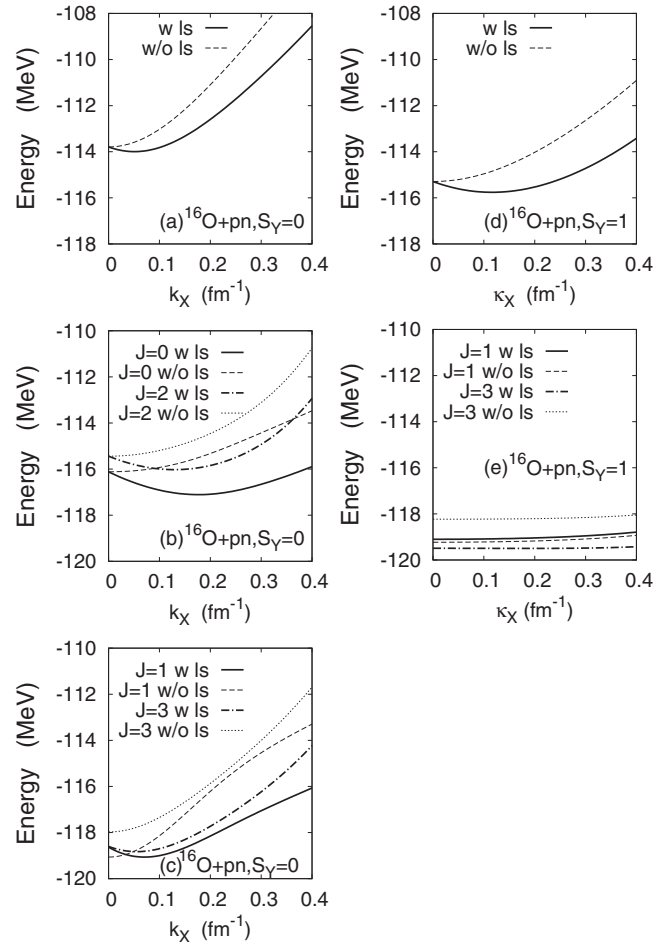

FIG. 6. The energy of the $\Phi_{^{16}\mathrm{O}+pn}(\boldsymbol{R}_1,\boldsymbol{R}_2)$ wave function for the $\uparrow_Y\downarrow_Y$ pair of two nucleons boosted in the opposite direction and that for $\uparrow_Y\uparrow_Y$ pair of two nucleons boosted in the same direction. The parameters $\boldsymbol{R}_1 = (ik_X/2\nu,0,D_g)$ and $\boldsymbol{R}_2 = (-ik_X/2\nu,0,D_g)$ are used for the $\uparrow_Y\downarrow_Y$ pair, and $\boldsymbol{R}_1 = (i\kappa_X/2\nu,0,D_g)$ and $\boldsymbol{R}_2 = (i\kappa_X/2\nu,0,D_g)$ are used for the $\uparrow_Y\uparrow_Y$ pair. D_g is fixed to be 2 fm. (Left) The energy for the $\uparrow_Y\downarrow_Y$ pn pair of (a) the intrinsic state without the J^π projection, (b) the $J^\pi = 0^+$ and 2^+ projected states with $T = 1$, and (c) the $J^\pi = 1^+$ and 3^+ projected states with $T = 0$. (Right) The energy for the $\uparrow_Y\uparrow_Y$ pn pair of (d) the intrinsic state and (e) the $J^\pi = 1^+$ and 3^+ projected states with $T = 0$. The bh125 interactions with and without the spin-orbit force are used.

in the pair. As a result, the finite k_X state is favored and the large energy gain is obtained in the spin-orbit potential in the $T = 1$, $J^\pi = 0^+$ and 2^+ states. The $J^\pi = 0^+$ and 2^+ states with the finite k_X receive similar effects of the spin-orbit force to each other. This is the reason why the 0^+-2^+ level spacing is almost unchanged in the GCM calculations with and without the spin-orbit force, as described previously in Sec. III (Fig. 3).

However, in the $T = 0$, $J^\pi = 1^+$ state for the $\uparrow_Y\downarrow_Y$ pair, the energy without the spin-orbit force rapidly increases as k_X increases, indicating the large internal energy loss in the pair as shown in Fig. 6(c). It means that the finite k_X states are unfavored in the $T = 0$, $J^\pi = 1^+$ state. In the results with the spin-orbit force, the internal energy loss compensates the spin-orbit potential gain in the finite k_X state. As a result, the

k_X value for the energy minimum with the spin-orbit force is small compared with the $T = 1$ states. Moreover, there is only a small difference between the energy minima for the results with and without the spin-orbit force. Also in the $T = 0$, $J^\pi = 3^+$ state, the rapid increase of the energy curve without the spin-orbit shows the large internal energy loss in the pair and indicates that the finite k_X states are not so favored. Namely, for the $T = 0$ states, the parity mixing in the pair does not contribute so much to the total energy gain in the spin-orbit potential. It should be commented that the $T = 0$, $J^\pi = 3^+$ state at $k_X = 0$ gains the spin-orbit force significantly because it is the $S = 1$ state coupling mainly with the $L = 2$ wave of the pair c.m. motion and feels the attractive spin-orbit potential. In other words, the $J^\pi = 3^+$ projected state of the $T = 0$ pair gains the spin-orbit force without the internal structure change of the pair consistently to the rotation boost in the intrinsic frame. It is different from the $T = 0$, $J^\pi = 1^+$ state at $k_X = 0$ of the pure $S = 1$ state coupling mainly with the $L = 0$ wave of the pair c.m. motion which feels almost no spin-orbit potential.

Let us discuss the κ_X dependence of the energy for the $T = 0$ $\uparrow_Y\uparrow_Y$ pair before and after the J^π projection. Note that the J^π projected states for the $\uparrow_Y\uparrow_Y$ pair are almost equivalent to the $T = 0$, J^π projected states for the $\uparrow_Y\downarrow_Y$ pair with $k_X = 0$ because both of them are pure $S = 1$ states having the ideal $(0s)^2$ pn pair. We show in Figs. 6(d) and 6(e) the energies of the intrinsic and the J^π projected states of $\Phi_{^{16}\mathrm{O}+pn}(\boldsymbol{R}_1, \boldsymbol{R}_2)$ for the $\uparrow_Y\uparrow_Y$ pair with the parameters $\boldsymbol{R}_1 = \boldsymbol{R}_2 = (i\kappa_X/2\nu, 0, D_g)$ ($D_g = 2$ fm), which corresponds to the rotation boost of the $T = 0$ $(0s)^2$ pair around the core. When the spin-orbit force is switched on, the energy minimum position of the intrinsic state shifts to the finite κ_X region, indicating the rotational excitation of the pair by the spin-orbit field in the intrinsic frame [see Fig. 6(d)]. Because κ_X changes only the proportion of the J^π components contained in the intrinsic state, the J^π projected energy does not depend on κ_X, as shown in Fig. 6(e) of the $J^\pi = 1^+$ and 3^+ projected energies for the $\uparrow_Y\uparrow_Y$ pair. In the projection, we choose the total angular momentum aligned to the intrinsic spin orientation in the projection as $J_Y = J$.

Let us come back to the $\uparrow_Y\downarrow_Y$ pn pair around the ^{16}O core. We discuss the D_g dependence as well as the k_X dependence of the energies of the $T = 1$, $J^\pi = 0^+$ and $T = 0$, $J^\pi = 1^+$ states projected from $\Phi_{^{16}\mathrm{O}+pn}(\boldsymbol{R}_1, \boldsymbol{R}_2)$ for the $\uparrow_Y\downarrow_Y$ pn pair. We use the parametrization $\boldsymbol{R}_1 = (ik_X/2\nu, 0, D_g)$ and $\boldsymbol{R}_2 = (-ik_X/2\nu, 0, D_g)$. The energies with and without the spin-orbit force are shown in Fig. 7 for the $T = 1$, $J^\pi = 0^+$ state and in Fig. 8 for the $T = 0$, $J^\pi = 1^+$ state. The contribution of the spin-orbit force evaluated by the energy difference with and without the spin-orbit force is also shown. As shown in the bottom panels of Figs. 7 and 8, the spin-orbit force contribution is attractive in the finite k_X region in both states, and the k_X dependence of the attraction is not so different between the 0^+ state and the 1^+ state at least in $D_g \leqslant 2$ fm region. The remarkable difference between the 0^+ and 1^+ states is found in the energy without the spin-orbit force. In contrast to the large energy loss of the 1^+ state in the finite k_X region, the energy loss of the 0^+ state is milder. As a result, in the total energy with the spin-orbit force, the minimum energy state for the 0^+ state appears in the finite k_X region and shows the significant reduction of the total energy because of the spin-orbit force.

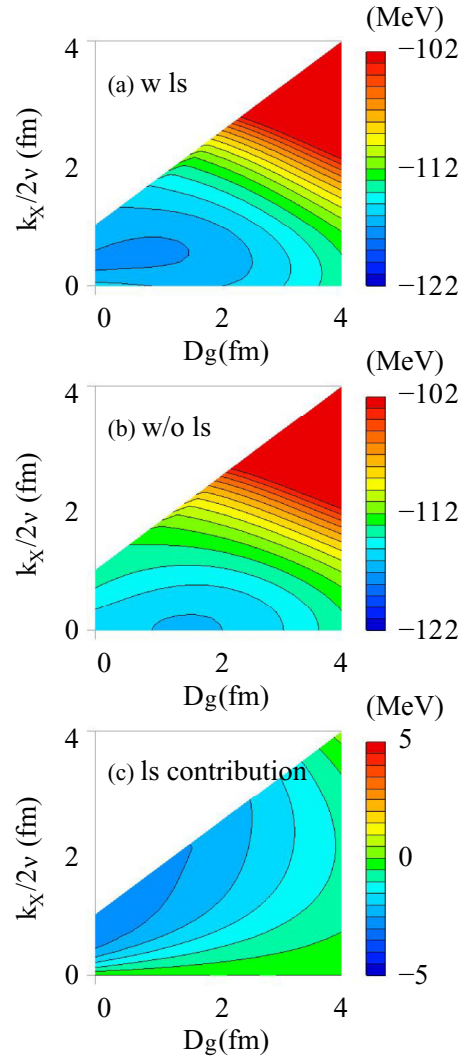

FIG. 7. (Color online) k_X and D_g dependence of the energy of the $\Phi_{^{16}\mathrm{O}+pn}$ wave function for the $\uparrow_Y\downarrow_Y$ pn pair projected onto the $T = 1$, $J^\pi = 0^+$ state. The energy (a) with the spin-orbit force and (b) without the spin-orbit force, and (c) the contribution of the spin-orbit force evaluated by the energy difference between with and without the spin-orbit force.

Thus, the parity symmetry is broken in the $T = 1$ pn pair by the spin-orbit field. In contrast, for the 1^+ state, the energy minimum state in the total energy exists near the $k_X = 0$ line, suggesting smaller symmetry breaking in the $T = 0$ pn pair because of the large energy loss in the finite k_X region.

As discussed in the previous section, the GCM calculation shows the smaller odd-parity component $\mathcal{P}_{\mathrm{odd}}$ of the pn pair in the $T = 0$, $J^\pi = 1^+$ state than that in the $T = 1$, $J^\pi = 0^+$ state (see Table I). It is consistent with the above analysis of the k_X dependence of the energy with and without the spin-orbit force. The feature that the $T = 0$, $J^\pi = 1^+$ state is not favored in the spin-orbit potential originates in the internal energy loss caused by the parity mixing in the $T = 0$ pair. Although the k_X dependence of the spin-orbit contribution is not so different between the 1^+ and 0^+ states, the internal energy increases rapidly in the $T = 0$, $J^\pi = 1^+$ state than in

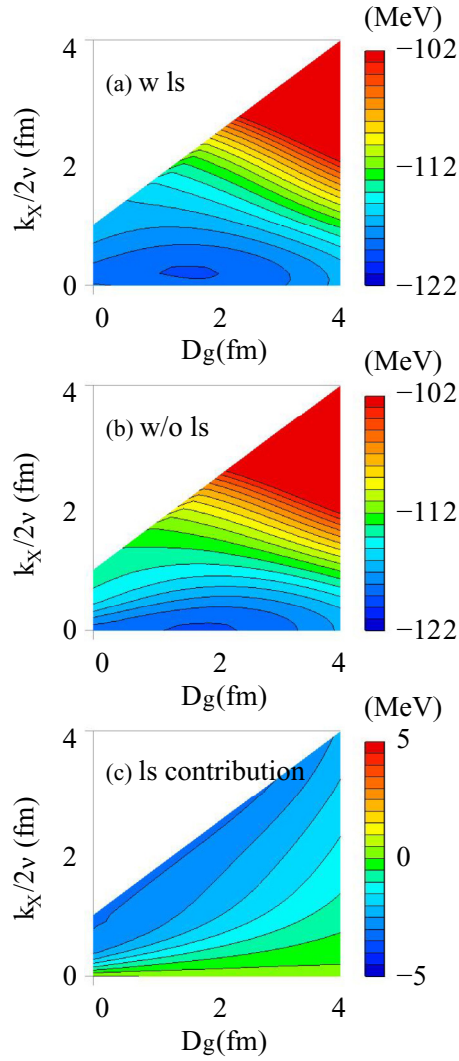

FIG. 8. (Color online) k_X and D_g dependence of the energy of the $\Phi_{^{16}\mathrm{O}+pn}$ wave function for the $\uparrow_Y\downarrow_Y pn$ pair projected onto the $T=0$, $J^\pi=1^+$ state. The energy (a) with the spin-orbit force and (b) without the spin-orbit force, and (c) the contribution of the spin-orbit force evaluated by the energy difference between with and without the spin-orbit force.

the $T=1$, $J^\pi=0^+$ state as k_X increases even in the case with the equal ^{3}E and ^{1}E central forces. As explained before, for the $\uparrow_Y\downarrow_Y$ pair in the spin-orbit potential, the finite k_X is favored to gain the spin-orbit potential energy by roughly $-2\frac{\tilde{U}_{ls}D_g}{2}k_X$ in the intrinsic frame. However, the finite k_X inevitably causes the internal energy loss because of the mixing of the odd-parity component in the pair. The $T=1$ and $T=0$ components of the $\uparrow_Y\downarrow_Y$ pair are decomposed by the $K=0$ and $K=1$ projections, respectively. For a given finite value of k_X, the internal energy loss of the pair is less in the $T=1$ pair than in the $T=0$ pair because the odd-parity mixing becomes about half of the intrinsic state in the $K=0$ projection for the $T=1$ component but it is not the case in the $K=1$ projection for the $T=0$ component, as explained in Appendix A. This means that, the finite k_X state is unlikely in the $T=0$ pair because of the larger internal energy loss than in the $T=1$ pair though the

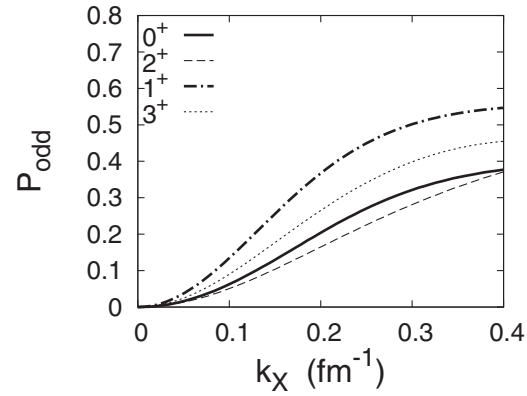

FIG. 9. k_X dependence of the odd-parity component $\mathcal{P}_{\mathrm{odd}}$ in the $\Phi_{^{16}\mathrm{O}+pn}$ wave function for the $\uparrow_Y\downarrow_Y pn$ pair projected onto the $T=1$, $J^\pi=0^+$ and 2^+ states and the $T=0$, $J^\pi=1^+$ and 3^+ states. D_g is fixed to be 2 fm.

k_X dependence of the spin-orbit potential energy gain is almost equal in the $T=1$ and $T=0$ components. As a result, in the energy minimum $T=0$, $J^\pi=1^+$ state with the spin-orbit potential, the parity mixing is suppressed and the total energy gain due to the spin-orbit potential is small.

We compare the k_X dependence of the odd-parity component $\mathcal{P}_{\mathrm{odd}}$ in the $T=1$ and $T=0$ states projected from $\Phi_{^{16}\mathrm{O}+pn}$ wave function for the $\uparrow_Y\downarrow_Y$ pair in Fig. 9. We use the parametrization $\boldsymbol{R}_1=(ik_X/2\nu,0,D_g)$ and $\boldsymbol{R}_2=(-ik_X/2\nu,0,D_g)$ with the fixed $D_g=2$ fm. It is found that, as k_X increases, the odd-parity component in the $T=0$, $J^\pi=1^+$ state increases more rapidly than that in the $T=1$, $J^\pi=0^+$ state. In the small k_X region, the odd-parity component in the $T=1$, $J^\pi=0^+$ state is about half of that in the $T=0$, $J^\pi=1^+$ consistently with the reduction of the odd-parity component in the K projection described in Appendix A. The increase of the odd-parity component directly causes the internal energy loss of the pair. This is consistent with the arguments of Refs. [12,15–17] discussed from the mean-field picture that the $T=0$ pairing is unfavored because of the small overlap between the jj coupling pair and the LS coupling pair in the $T=0$, $J^\pi=1^+$ channel than the $T=1$, $J^\pi=0^+$ channel.

V. FOUR-NUCLEON CORRELATION AT NUCLEAR SURFACE

We discuss here the effect of the spin-orbit force on the α cluster breaking in analogy to the effect on the dinucleon pair. As discussed before, the spin-orbit force changes the internal structure of the $T=1$ $\uparrow_Y\downarrow_Y$ pair and the c.m. motion of the $T=0$ $\uparrow_Y\uparrow_Y$ pair in the intrinsic frame. The former contributes to the energy gain in the $T=1$, $J^\pi=0^+$ state and the latter affects the energy gain of the $T=1$, $J^\pi=3^+$ and 5^+ states. In contrast, the spin-orbit force gives minor contribution to the energy of the $T=0$, $J^\pi=1^+$ state. For the α cluster around the ^{16}O in the $T=0$, $J^\pi=0^+$ state, a $\uparrow_Y\uparrow_Y$ pn pair in a finite L wave can couple with a $\downarrow_Y\downarrow_Y$ pn pair in the L wave in the opposite direction to form the α cluster in the total orbital angular momentum $L=0$ state (see Fig. 10). Therefore, the α cluster in the $L=0$ wave may gain

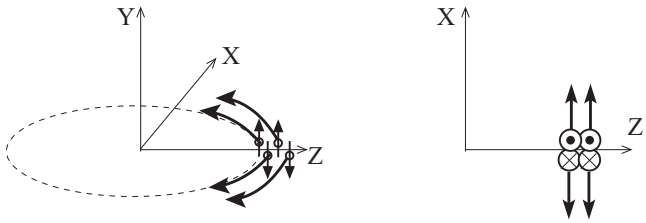

FIG. 10. Schematic figures for four nucleons in the spin-orbit potential at the nuclear surface.

the spin-orbit potential energy involving the cluster breaking from the $(0s)^4$ configuration. It may be useful to discuss the effect of the spin-orbit force on the breaking in analogy to the effect on the pn pair, although the α cluster breaking is expected to be suppressed because of the larger binding energy of the α cluster than the pn pair.

We perform an analysis of four nucleons around the ^{16}O by using the $^{16}\mathrm{O}+4N$ wave function given in Eq. (23) in a way similar to how we analyze the pn pair. The adopted effective nuclear interaction is the bh125 interaction with and without the spin-orbit force. We consider the α cluster localized around the position $(0,0,D_g)$ on the Z axis,

$$\boldsymbol{R}_g \equiv \frac{\boldsymbol{R}_1+\boldsymbol{R}_2+\boldsymbol{R}_3+\boldsymbol{R}_4}{4} = (0,0,D_g), \tag{35}$$

with a real value D_g for the distance from the ^{16}O core. If we take $\boldsymbol{R}_1=\boldsymbol{R}_2=\boldsymbol{R}_3=\boldsymbol{R}_4=\boldsymbol{R}_g$, four nucleons form the $(0s)^4$ α cluster.

Let us consider the α cluster breaking in the spin-orbit field at the nuclear surface. We fix the Z component $R_{jZ}=D_g$ and vary R_{jX} and R_{jY} to get the energy minimum state under the constraints,

$$\frac{R_{1X}+R_{2X}}{2} = \frac{R_{3X}+R_{4X}}{2} = 0, \tag{36}$$

$$\frac{R_{1Y}+R_{2Y}}{2} = \frac{R_{3Y}+R_{4Y}}{2} = 0. \tag{37}$$

This is equivalent to the constraints $R_{gX}=0$ and $R_{gY}=0$ without the dipole excitation. This model is regarded as a special case of the d-constraint method in antisymmetrized molecular dynamics (AMD) [35]. After the energy variation, we obtain the optimum parameter set R_{jX} and R_{jY} which minimizes the energy of the wave function $\Phi_{^{16}\mathrm{O}+4N}(\boldsymbol{R}_1,\boldsymbol{R}_2,\boldsymbol{R}_3,\boldsymbol{R}_4)$ under the constraints.

We first perform the variation with respect to the intrinsic energy without the parity and the total-angular-momentum projections. In the result without the spin-orbit force, the optimum parameters in the minimum energy state are found to be

$$\boldsymbol{R}_1=\boldsymbol{R}_2=\boldsymbol{R}_3=\boldsymbol{R}_4=(0,0,D_g), \tag{38}$$

indicating that the ideal $(0s)^4$ α cluster is formed at the surface. When the spin-orbit force is switched on, the optimum $\boldsymbol{R}_j$ in the minimum energy state has the finite imaginary part as $\boldsymbol{R}_1=\boldsymbol{R}_3\approx(ik_X/2\nu,0.D_g)$ and $\boldsymbol{R}_2=\boldsymbol{R}_4\approx(-ik_X/2\nu,0.D_g)$. It means that spin-up and -down nucleons in the α cluster are boosted in the opposite direction along the X axis in the spin-orbit field from the ^{16}O as shown in Fig. 10. The present result without the projections is consistent with the cluster breaking discussed in the AMD calculation of ^{28}Si [36]. It is also consistent with the simplified model for the α-cluster breaking proposed by Itagaki *et al.* [37]. The parameter k_X in the present model relates to the parameter Λ introduced in the simplified model as $\Lambda=k_X/2\nu D_g$, and it is regarded as the order parameter which indicates the cluster breaking at the nuclear surface. In Fig. 11(a), the D_g dependence of the nucleon momentum k_{jX} obtained by the energy variation without the projections is shown. $k_X=k_{1X}=-k_{2X}=k_{3X}=-k_{4X}$ is largest at $D_g=2$ fm and it becomes small with the increase of the distance D_g from the core.

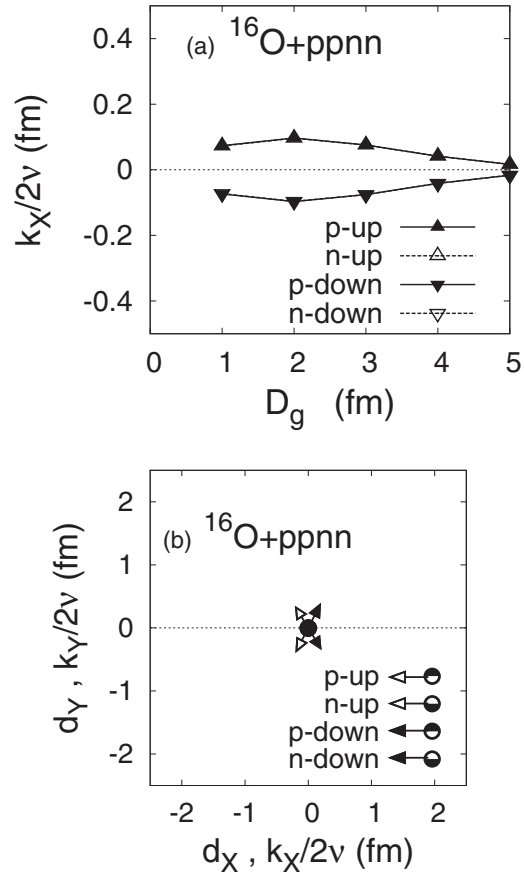

FIG. 11. Optimized $\boldsymbol{R}_j$ in $\Phi_{^{16}\mathrm{O}+4N}$ for the α cluster around the ^{16}O core. (a) D_g dependence of k_{jX} obtained by the energy variation without the projection. The k_{jX} values for the $\uparrow_Y$ and $\downarrow_Y$ neutrons are consistent with the values for protons. (b) $\boldsymbol{R}_j$ obtained by the VAP calculation for the $J^\pi=0^+$ state are projected onto the XY plane. The real parts (d_{jX},d_{jY}) for four nucleons are shown as the position on the XY plane, and they are located at the origin in the present result. The imaginary parts $(k_{jX}/2\nu,k_{jY}/2\nu)$ for four nucleons are illustrated by the lengths of the arrows. The bh125 interaction with the spin-orbit force is used.

We also perform the energy variation for the $J^\pi=0^+$ state projected from the $\Phi_{^{16}\mathrm{O}+4N}$ wave function with $D_g=2$ fm. The parameters $\boldsymbol{R}_j$ for nucleons in the α cluster obtained by the VAP are shown in Fig. 11(b). In the VAP result, k_{jY} is also finite as well as k_{jX}, indicating further breaking of the $(0s)^4$ α

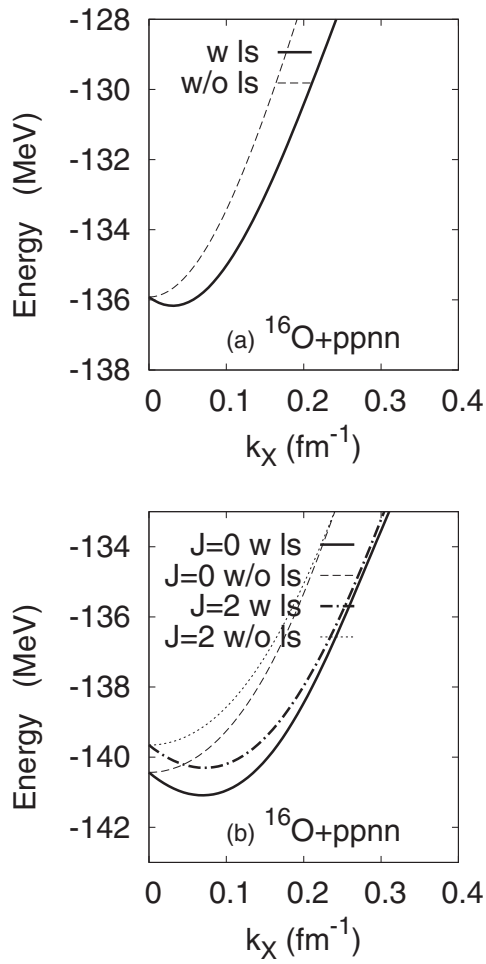

FIG. 12. k_X dependence of the energy of the $\Phi_{^{16}O+4N}$ wave function with $D_g = 2$ fm. (a) The energy of the intrinsic state and (b) that of the $J^\pi = 0^+$ and 2^+ projected states. The bh125 interactions with and without the spin-orbit force are used.

cluster in addition to the breaking described by the parameter k_{jX}. Qualitatively, the breaking of the $(0s)^4$ α cluster breaking around ^{16}O core is similar to that of the $(0s)^2$ pn pair in the $T = 0$, $J^\pi = 0^+$ state. However, quantitatively, the α cluster breaking is smaller than the pn pair breaking because the α cluster has the larger internal binding energy than the pn pair and its breaking is unlikely.

To see the energy gain of the spin-orbit potential in $\Phi_{^{16}O+4N}$ with the cluster breaking, we analyze the k_X dependence of the energy assuming $\mathrm{Re}[R_{jX}] = 0$ and $R_{jY} = 0$ for simplicity. The calculated energies of the body-fixed intrinsic state and that of the 0^+ state are shown in Fig. 12. It is found that the energy minimum shifts to the finite k_X region, indicating that the α breaking occurs because of the spin-orbit field, in particular, in the $J^\pi = 0$ projected states. Compared with the k_X dependence of the energy of the $\uparrow_Y\downarrow_Y$ pn pair, the energy without the spin-orbit force is very steep with respect to the cluster-breaking parameter k_X because of the large internal energy loss of the α cluster. As a result, the α cluster breaking in the 0^+ state is not as significant as the $\uparrow_Y\downarrow_Y$ pn pair though the spin-orbit force gives some attractive effect in the finite k_X region.

It is interesting to consider the analogy of the effect of the spin-orbit force on the α cluster breaking with that on the pn pair discussed in the previous section. The α cluster is composed of four nucleons, spin-up and -down protons and neutrons. In the spin-orbit field, the spin-up and -down nucleons are boosted in the opposite direction. It means that, in the body-fixed frame, the α cluster can be regarded as a composite of the $\uparrow_Y\uparrow_Y$ pn pair and the $\downarrow_Y\downarrow_Y$ pn pair, which are boosted in the opposite direction (see Fig. 10). We also consider an alternative interpretation of the α cluster as the composite of two $T = 1$ pairs, $\uparrow_Y\downarrow_Y$ pp and nn pairs. Then, the behavior of the $T = 1$ pairs in the α cluster is qualitatively consistent with the $\uparrow_Y\downarrow_Y$ pn pair having the parity mixing in the intrinsic frame discussed before.

It should be commented that one should not directly link the $J^\pi = 0^+$ pp and $J^\pi = 0^+$ nn pairs with the α cluster because the α cluster consists of correlating two pairs and it contains not only $J^\pi = 0^+$ pairs but also finite J pairs. In other words, $J^\pi = 0^+$ pp and nn pairs have no spacial correlation between each other and they are different from the correlating four nucleons in the α cluster. We can connect the $4N$ correlation with the $2N$ correlation only in the intrinsic body-fixed frame before the J projection or with the correlating pairs having finite momenta.

VI. SUMMARY

We investigated the structure of ^{18}F with the microscopic wave function based on the three-body $^{16}\mathrm{O} + p + n$ model to discuss the behavior of the pn pair around the ^{16}O. Particular attention was paid to the effect of the spin-orbit force on the pn pair behavior.

In the GCM calculation, the $T = 0$ energy spectra of $J^\pi = 1^+$, 3^+, and 5^+ states and the $T = 1$ spectra of $J^\pi = 0^+$, 2^+ states in ^{18}F are described reasonably. The spin-orbit potential from the core plays an important role in the energy spectra. The spin-orbit potential energy gain is largest in the $T = 0$, $J^\pi = 5^+$ state while it is small in the $T = 0$, $J^\pi = 1^+$ state. The significant energy gain of the spin-orbit potential is caused in the $T = 1$, $J^\pi = 0^+$states.

We discuss the effect of the spin-orbit force on the $T = 0$ and $T = 1$ pn pair around the ^{16}O based on the dinucleon picture. For the parallel-spin $\uparrow_Y\uparrow_Y$ pair for the $T = 0$ states, the spin-orbit potential boosts the c.m. motion of the pair in the rotational mode (the rotation boost of the pair), keeping the internal structure of the pair unchanged. It results in the larger energy gain in the higher spin J states in the $T = 0$ spectra. For the antiparallel-spin $\uparrow_Y\downarrow_Y$ pair in the body-fixed frame, the parity mixing in the pair occurs because of the external spin-orbit field. In other words, the pn pair gains the spin-orbit potential energy involving the odd-parity mixing, i.e., the symmetry breaking in the pair. The spin-orbit potential energy gain with the odd-parity mixing is efficient in the $T = 1$ pair in the $J^\pi = 0^+$ state, but it is not so efficient in the $T = 0$ pair in the $J^\pi = 1^+$ state because of the large internal energy loss of the $T = 0$ pair. The main origin of the smaller internal energy loss of the $T = 1$ pair than the $T = 0$ pair is that the odd-parity component is reduced in the projection onto the $T = 1$, $J^\pi = 0^+$ eigenstate but there is no reduction in

the $T = 0$, $J^\pi = 1^+$ projection. Thus, the parity mixing is likely in the $T = 1$ pair in the $J^\pi = 0^+$ state but it is unlikely in the $T = 0$ pair in the $J^\pi = 1^+$ state. Because the $T = 1$, $J^\pi = 0^+$ pair is favored by the spin-orbit potential while the $T = 0$, $J^\pi = 1^+$ pair is not favored, the $T = 1$, $J^\pi = 0^+$ state comes down to the low-energy region though the $T = 0$, $J^\pi = 1^+$ state is still the lowest state in ^{18}F because of the stronger ^{3}E nuclear force than the ^{1}E force.

The mechanism of the unfavorable $T = 0$ pair in the spin-orbit potential is consistent with the discussions in Refs. [5,12,15–18]. One of the new standpoints in the present work is that we focus on the internal pair wave function and discuss its change involving the odd-parity mixing because of the spin-orbit force. In the present picture, the parity mixing in the pair is regarded as the symmetry breaking in the pair by the symmetry variant external spin-orbit field.

ACKNOWLEDGMENTS

The authors would like to thank Dr. Itagaki and Dr. Tanimura for useful discussions. The computational calculations of this work were performed by using the supercomputers at Yukawa Institute for Theoretical Physics. This work was supported by Japan Society for the Promotion of Science KAKENHI Grants No. 22540275 and No. 26400270.

APPENDIX A: DINUCLEON CLUSTER PICTURE AND PARITY MIXING IN THE PAIR

We consider two nucleons around the core nucleus and describe how the parity symmetry in the pair is broken by the spin-orbit external field.

We introduce a simplified potential model where all core effects are assumed to be renormalized in the one-body effective central and spin-orbit potentials, while the recoil effect is omitted. In the simplified model, the Hamiltonian is given as

$$H = t_1 + t_2 + U_c(r_1) + U_c(r_2) + U_{\rm ls}(r_1)\boldsymbol{l}_1 \cdot \boldsymbol{s}_1 + U_{\rm ls}(r_2)\boldsymbol{l}_2 \cdot \boldsymbol{s}_2 + v_{NN}(r), \tag{A1}$$

which describes interacting two nucleons in the external field from the core. We first explain the mean-field picture and then describe the dinucleon picture based on this model for a pair around the core.

In the mean-field approximation, the Hamiltonian is rewritten as

$$H = h_1 + h_2 + v_{NN}(r), \tag{A2}$$

$$h_i = t_i + U_i, \tag{A3}$$

$$U_i = U_c(r_i) + U_{\rm ls}(r_i)\boldsymbol{l}_i \cdot \boldsymbol{s}_i. \tag{A4}$$

The one-body parts of the Hamiltonian is considered to be the unperturbative Hamiltonian $H_0 = h_1 + h_2$ and the residual interaction $H' = v_{NN}$ is regarded as the perturbative Hamiltonian which causes the two-body correlation. In the leading term H_0, two nucleons behave as independent particles in the mean field U_i containing the spin-orbit potential, and the correlated wave function is expressed by the linear combination of the single-particle configurations. It corresponds to the expression of the jj coupling scheme.

When we respect the internal symmetry of the pair, the picture based on the LS coupling scheme is useful rather than the jj coupling scheme because the Hamiltonian without the spin-orbit potential has the symmetry for the internal parity of the pair, which is explicitly broken by the spin-orbit potential. For the LS coupling picture, we consider another choice of the unperturbative Hamiltonian by regarding the spin-orbit potential as the perturbative external field for two nucleons,

$$H = \tilde{H}_0 + \tilde{H}', \tag{A5}$$

$$\tilde{H}_0 = t_1 + t_2 + U_c(r_1) + U_c(r_2) + v_{NN}(r), \tag{A6}$$

$$\tilde{H}' = U_{\rm ls}(r_1)\boldsymbol{l}_1 \cdot \boldsymbol{s}_1 + U_{\rm ls}(r_2)\boldsymbol{l}_2 \cdot \boldsymbol{s}_2. \tag{A7}$$

In $\tilde{H}_0$, two nucleons bound in the central potential form the pn pair at the surface because of the S-wave attraction of the nuclear force v_{NN}. The $(TS) = (01)$ and (10) pairs are formed by the attractions in the ^{3}E and ^{1}E channels, respectively. Because the total intrinsic spin S and the total orbital angular momentum L are conserved, this picture is called the "LS coupling" scheme. In the internal wave function of the pair, the parity transformation $\boldsymbol{r} \to -\boldsymbol{r}$ ($\boldsymbol{r} \equiv \boldsymbol{r}_1 - \boldsymbol{r}_2$) is equivalent to the exchange $\boldsymbol{r}_1 \leftrightarrow \boldsymbol{r}_2$, and therefore, the internal parity of the pair is conserved in the unperturbative system because $\tilde{H}_0$ is invariant under the internal parity transformation, $\boldsymbol{r}_1 \leftrightarrow \boldsymbol{r}_2$.

Based on the two-nucleon pair with the parity symmetry in the LS coupling scheme, we consider the spin-orbit potential as the perturbative external field that explicitly breaks the parity symmetry in the pair. The total Hamiltonian $H = \tilde{H}_0 + \tilde{H}'$ is no longer invariant under the transformation $\boldsymbol{r}_1 \leftrightarrow \boldsymbol{r}_2$. As a result, the odd-parity component mixes in the dominant even-parity component in the internal pair wave function. Because of the Fermi statistics, it means that the spin-singlet odd (^{1}O) component is mixed in the ^{3}E component in the $T = 0$ pair and the ^{3}O component is mixed in the ^{1}E component in the $T = 1$ pair.

To consider the breaking of the parity symmetry in the pn pair, we discuss a $\uparrow_Y\downarrow_Y$ pn pair localized around a certain position $(0,0,D_g)$ on the Z axis. Ignoring the degree of freedom along Z axis for simplicity, we look only into the two-dimensional (2D) problem on the XY plane passing through $(0,0,D_g)$. For a simple explanation of the parity mixing in the pair due to the spin-orbit potential, we introduce a toy model which mimics the 2D problem for the pair. Namely, we assume the 2D H.O. potential around the origin of the coordinates $\boldsymbol{\rho} = (X,Y)$ and add the perturbative field contributed by the spin-orbit potential:

$$H_{\rm 2D} = H^{(0)}_{\rm 2D} + H'_{\rm 2D}, \tag{A8}$$

$$H^{(0)}_{\rm 2D} = \frac{1}{2m}\left(p_{1X}^2 + p_{1Y}^2\right) + \frac{m\omega^2}{2}\boldsymbol{\rho}_1^2 + \frac{1}{2m}\left(p_{2X}^2 + p_{2Y}^2\right) + \frac{m\omega^2}{2}\boldsymbol{\rho}_2^2, \tag{A9}$$

$$H'_{\rm 2D} = -\frac{\bar{V}_{\rm ls}}{\hbar}(p_{1X}s_{1Y} - p_{1Y}s_{1X}) - \frac{\bar{V}_{\rm ls}}{\hbar}(p_{2X}s_{2Y} - p_{2Y}s_{2X}). \tag{A10}$$

Here the contributions from the nucleon-nucleon interaction as well as the central potential in $\tilde{H}_0$ are assumed to be renormalized in the H.O.-type mean potential $H^{(0)}_{\rm 2D}$. The spin-orbit potential contribution is approximated by the averaged strength $-\bar{V}_{\rm ls} \approx U_{\rm ls}(D_g)D_g$, assuming the coordinate $\boldsymbol{r}_i$ in the spin-orbit potential to be constant $\boldsymbol{r}_i \approx (0,0,D_g)$. $\bar{V}_{\rm ls}$ is a positive constant value. The H.O. assumption for the unperturbative potential is not essential but it can be another potential form with the 2D-rotational symmetry (the axial symmetry in 3D). The present H.O. assumption is used just for the convenience that the internal wave function and the c.m. wave function of the pair are separable in the lowest state of the H.O. potential.

The lowest state of two nucleons, $\uparrow_Y$ p and $\uparrow_Y$ n, for $H^{\rm 2D}_0$ is the $(0s)^2_{\rm 2D}$ configuration in 2D,

$$\Phi_0(1,2) = \tfrac{1}{2}\mathcal{A}\{\phi_0(\boldsymbol{\rho}_1)\chi_{p\uparrow_Y}\phi_0(\boldsymbol{\rho}_2)\chi_{n\downarrow_Y}\}, \tag{A11}$$

$$\phi_0(\boldsymbol{\rho}_i) = \phi^{\rm 2D}_{0s}(b;\boldsymbol{\rho}_i), \tag{A12}$$

$$b = \sqrt{\frac{\hbar}{m\omega}}, \tag{A13}$$

where $\phi^{\rm 2D}_{0s}(b;\boldsymbol{\rho})$ is the function for the $0s$ state of the 2D H.O. with the size parameter b,

$$\phi^{\rm 2D}_{0s}(b;\boldsymbol{\rho}) \equiv \left(\frac{1}{\pi b^2}\right)^{1/2} e^{-\frac{\rho^2}{2b^2}}. \tag{A14}$$

The spatial part of the wave function of the $(0s)^2_{\rm 2D}$ state is expressed by a product of the c.m. wave function $\phi^{\rm 2D}_{g,0}$ and the internal wave function $\phi^{\rm 2D}_{{\rm in},0}$,

$$\phi_0(\boldsymbol{\rho}_1)\phi_0(\boldsymbol{\rho}_2) = \phi_{g,0}(\boldsymbol{\rho}_g)\phi_{{\rm in},0}(\boldsymbol{\rho}), \tag{A15}$$

$$\phi^{\rm 2D}_{g,0} = \phi^{\rm 2D}_{0s}\left(\frac{b}{\sqrt{2}};\boldsymbol{\rho}_g\right), \tag{A16}$$

$$\phi^{\rm 2D}_{{\rm in},0} = \phi^{\rm 2D}_{0s}(\sqrt{2}b;\boldsymbol{\rho}), \tag{A17}$$

with the c.m. and relative coordinates, $\boldsymbol{r}_g \equiv (\boldsymbol{r}_1+\boldsymbol{r}_2)/2$ and $\boldsymbol{r} \equiv \boldsymbol{r}_1 - \boldsymbol{r}_2$ of the pair. Needless to say, the internal wave function $\phi^{\rm 2D}_{{\rm in},0}$ of the pair contains only the even-parity component.

Because of the spin-momentum coupling term $H'_{\rm 2D}$ originating in the spin-orbit potential, the parity mixing occurs in the $\uparrow_Y\downarrow_Y$ pair. The total Hamiltonian for the $\uparrow_Y\downarrow_Y$ pair can be written as

$$H^{\rm 2D} = \frac{1}{2m}\left\{(p_{1X}-\hbar k_X)^2 + p^2_{1Y}\right\} + \frac{m\omega^2}{2}\boldsymbol{\rho}_1^2 + \frac{1}{2m}\left\{(p_{2X}+\hbar k_X)^2 + p^2_{2Y}\right\} + \frac{m\omega^2}{2}\boldsymbol{\rho}_2^2 + C, \tag{A18}$$

$$k_X \equiv \frac{m}{2\hbar^2}\bar{V}_{\rm ls}, \tag{A19}$$

$$C = -\frac{m}{4\hbar^2}\bar{V}^2_{\rm ls}. \tag{A20}$$

The energy shift C of the lowest state is proportional to $\bar{V}^2_{\rm ls}$ instead of $\bar{V}_{\rm ls}$ because the leading order of the energy perturbation vanishes, $\langle\Phi_0|H'_{\rm 2D}|\Phi_0\rangle = 0$. Single-particle wave functions for the spin-up ($\uparrow_Y$) and -down ($\downarrow_Y$) nucleons in the lowest state are those shifted in the momentum space in the opposite direction along the X axis,

$$\phi(\boldsymbol{\rho}_1) = \left(\frac{1}{\pi b^2}\right)^{1/2} e^{-\frac{\rho_1^2}{2b^2}} e^{ik_X X_1}, \tag{A21}$$

$$\phi(\boldsymbol{\rho}_2) = \left(\frac{1}{\pi b^2}\right)^{1/2} e^{-\frac{\rho_2^2}{2b^2}} e^{-ik_X X_2}. \tag{A22}$$

In other words, two nucleons are boosted with the momentum k_X in the opposite direction by the spin-momentum coupling field. As a result the odd-parity mixing occurs in the internal wave function of the pair as

$$\phi(\boldsymbol{\rho}_1)\phi(\boldsymbol{\rho}_2) = \phi^{\rm 2D}_{g,0}(\boldsymbol{\rho}_g)\phi^{\rm 2D}_{\rm in}(\boldsymbol{\rho}), \tag{A23}$$

$$\phi^{\rm 2D}_{\rm in}(\rho) = \left(\frac{1}{2\pi b^2}\right)^{1/2} e^{-\frac{\rho^2}{4b^2}} e^{ik_X X} = \phi^{\rm 2D}_{0s}(\sqrt{2}b:\boldsymbol{\rho}) + ik_X b\phi^{\rm 2D}_{0p_X}(\sqrt{2}b;\boldsymbol{\rho}) + \mathcal{O}\left(k_X^2\right). \tag{A24}$$

Here $\phi^{\rm 2D}_{0p_X}$ indicates the $0p_X$ state in the 2D H.O. In the limit of the small perturbation, the odd-parity component is $k_X^2/4b^2 = m^2\bar{V}^2_{\rm ls}/16\hbar^4b^2$, which is proportional to the square of the strength of the spin-orbit field.

Clearly shown in this schematic model, the parity symmetry in the pair breaks because of the spin-orbit field. The order parameter k_X relating to the odd-parity component is determined by the competition between the spin-orbit potential energy gain and the energy cost to break the symmetry. The energy cost comes from the energy loss to excite the lowest $0p$ state to the $0p$ state in the pair, and it is proportional to the $0p$ mixing (parity mixing) component. In the following, we show that the ratio of the $0p$ component to the dominant $0s$ component in the pair changes in the $J_Z = K$ projection which is equivalent to the T projection. Namely, the $0p$ component is quenched in the $T = 1$ projection, resulting in the smaller internal energy loss in the $T = 1$ pair. Similar discussions can be found in Ref. [18].

The $\uparrow_Y\downarrow_Y$ pn pair contains $T = 0$ and $T = 1$ components as

$$\chi_{p\uparrow_Y}\chi_{n\downarrow_Y} = \frac{\mathcal{X}_{01}}{2} + \frac{\mathcal{X}_{10}}{2} + \frac{\mathcal{X}_{00}}{2} + \frac{\mathcal{X}_{11}}{2}, \tag{A25}$$

where $\mathcal{X}_{TS}$ is the isospin-spin TS state of two nucleons. The parity-mixed pn pair can be decomposed into $T = 0$ and $T = 1$ eigenstates as

$$\Phi(1,2) = \frac{1}{2}\mathcal{A}\{\phi(\boldsymbol{\rho}_1)\chi_{p\uparrow_Y}\phi(\boldsymbol{\rho}_2)\chi_{n\downarrow_Y}\} = \phi^{\rm 2D}_{g,0}(\boldsymbol{r}_g)\cdot\left\{\phi^{\rm 2D}_{0s}(\sqrt{2}b;\boldsymbol{\rho})\frac{\mathcal{X}_{01}}{2} + ik_X b\phi^{\rm 2D}_{0p_X}(\sqrt{2}b;\boldsymbol{\rho})\times\frac{\mathcal{X}_{00}}{2} + \phi^{\rm 2D}_{0s}(\sqrt{2}b;\boldsymbol{\rho})\frac{\mathcal{X}_{10}}{2} + ik_X b\phi^{\rm 2D}_{0p_X}(\sqrt{2}b;\boldsymbol{\rho})\frac{\mathcal{X}_{11}}{2}\right\} + \mathcal{O}\left(k_X^2\right). \tag{A26}$$

In the 2D system in the intrinsic frame, there is no difference in the ratio of the even-parity and odd-parity components between $T = 0$ and $T = 1$ states. However, because the

2D Hamiltonian has the rotational symmetry around the Z axis (the axial symmetry) and as a result of the symmetry restoration, the $J_Z = K$ eigenstate projected from the intrinsic state should be considered. The $K = 0$ and $K = \pm 1$ projected pairs correspond to the $T = 1$ and $T = 0$ pairs, respectively, and they are naively expected in the $T = 1$, $J^\pi = 0^+$ and $T = 1$, $J^\pi = 1^+$ states. Choosing the Z axis as the quantization axis, the orbital angular momentum $0p_X$ state can be rewritten in terms of $|ll_Z\rangle_l$ as

$$|0p_X\rangle = \frac{1}{\sqrt{2}}(|1-1\rangle_l - |1+1\rangle_l), \tag{A27}$$

and also the $S = 1$ component of the $S_Y = 0$ state in $\mathcal{X}_{T1}$ can be rewritten in terms of $|SS_Z\rangle_s$ as

$$|\mathcal{X}_{T1}\rangle = \frac{i}{\sqrt{2}}(|1-1\rangle_s + |1+1\rangle_s)|T\rangle. \tag{A28}$$

For the $T = 1$ pair, the odd-parity term $\phi^{\rm 2D}_{0p_X}(2b)\mathcal{X}_{11}$ can be decomposed by $|1-1\rangle_l|1-1\rangle_s$, $|1+1\rangle_l|1+1\rangle_s$, $|1-1\rangle_l|1+1\rangle_s$, and $|1+1\rangle_l|1-1\rangle_s$ components. It means that the odd-parity term of the $T = 1$ component contains the $K = 0$ and $K = 2$ components in equal weight, while the even-parity term $\phi^{\rm 2D}_{0s}(2b)\mathcal{X}_{10}$ contains only the $K = 0$ component. As a result, the odd-parity component is suppressed in the $K = 0$ projected state, and the ratio of the odd-parity to the even-parity components in the $T = 1$ pair is reduced to be half of the intrinsic state. However, for the $T = 0$ pair, there is no reduction of the odd-parity component in the $K = \pm 1$ projection, and the ratio in the $T = 0$ pair is the same as that in the intrinsic state. In other words, the even-parity component is relatively enhanced in the $K = 0$ projection for the $T = 1$ state, while such an enhancement of the even-parity component does not occur in the $K = \pm 1$ projection for the $T = 0$ state.

APPENDIX B: RELATION BETWEEN *pn* CLUSTER WAVE FUNCTION AND SHELL-MODEL WAVE FUNCTION

In this work, we use the three-body cluster model of $^{16}\mathrm{O} + p + n$ with the form of Gaussian wave packets for two nucleons. We here show that this wave function becomes an sd-shell configuration of the H.O. shell model in a certain limit.

In a basis cluster wave function $\Phi_{^{16}\mathrm{O}+pn}(\boldsymbol{R}_1, \boldsymbol{R}_2)$ of Eq. (1), the spatial part of the single-particle wave function for the ith valence nucleon is described with a Gaussian wave packet of Eq. (3),

$$\phi(\boldsymbol{R}_j; \boldsymbol{r}_i) = \left(\frac{2\nu}{\pi}\right)^{3/4} e^{-\nu(\boldsymbol{r}_i - \boldsymbol{R}_j)^2}. \tag{B1}$$

Using the expansion $e^{-t^2+2xt} = \sum_{n=0}^{\infty} H_n(x)t^n/n!$ with the Hermite polynomial $H_n(x)$, this Gaussian wave packet can be rewritten by an expansion of the H.O. shell-model single-particle wave function $(n_x,n_y,n_z)_{\rm ho}$ for the width parameter $b = 1/\sqrt{2\nu}$ as

$$\phi(\boldsymbol{R}_j; \boldsymbol{r}_i) = \sum_{n_x,n_y,n_z} \mathcal{N}_{n_x n_y n_z}(\boldsymbol{R}_j)(n_x,n_y,n_z)_{\rm ho}, \tag{B2}$$

$$\mathcal{N}_{n_x n_y n_z}(\boldsymbol{R}_j) = e^{-\frac{\nu}{2}\boldsymbol{R}_j^2} \prod_{\sigma=x,y,z} \left(\sqrt{\frac{\nu}{2}} R_{j\sigma}\right)^{n_\sigma} \frac{2^{n_\sigma/4}}{(n_\sigma!)^{3/4}}. \tag{B3}$$

Note that the coefficient $\mathcal{N}_{n_x n_y n_z}(\boldsymbol{R}_j)$ is the order of $|\boldsymbol{R}_j|^N$ ($N \equiv n_x + n_y + n_z$) in the small $|\boldsymbol{R}_j|$ limit.

Because $N \leqslant 1$ orbits are already occupied by nucleons in the ^{16}O core, only $N \geqslant 2$ orbits are allowed for valence nucleons in the the total wave function $\Phi_{^{16}\mathrm{O}+pn}(\boldsymbol{R}_1, \boldsymbol{R}_2)$. It means that $N \leqslant 1$ shell-model configurations vanish in the total wave function after the antisymmetrization and $N \geqslant 2$ configurations remains. Defining the orthogonal component of $\phi(\boldsymbol{R}_j; \boldsymbol{r}_i)$ to the forbidden $N \leqslant 1$ orbits as

$$\tilde{\phi}(\boldsymbol{R}_j; \boldsymbol{r}_i) = \sum_{N\geqslant 2} \mathcal{N}_{n_x n_y n_z}(\boldsymbol{R}_j)(n_x,n_y,n_z)_{\rm ho}, \tag{B4}$$

we can rewrite the $^{16}\mathrm{O} + p + n$ wave function as

$$\Phi_{^{16}\mathrm{O}+pn}(\boldsymbol{R}_1, \boldsymbol{R}_2) = \mathcal{A}\{\Phi_{^{16}\mathrm{O}}\tilde{\psi}_{p\sigma}(\boldsymbol{R}_1)\tilde{\psi}_{n\sigma'}(\boldsymbol{R}_2)\}, \tag{B5}$$

$$\tilde{\psi}_{\tau\sigma}(\boldsymbol{R}_j; \boldsymbol{r}_i) = \tilde{\phi}(\boldsymbol{R}_j; \boldsymbol{r}_i)\chi_{\tau\sigma}. \tag{B6}$$

In the limit of $|\boldsymbol{R}_j| \to 0$, the lowest order $\tilde{\phi}(\boldsymbol{R}_j; \boldsymbol{r}_i)$ term becomes dominant in $\tilde{\phi}(\boldsymbol{R}_j; \boldsymbol{r}_i)$ as

$$\tilde{\phi}(\boldsymbol{R}_j; \boldsymbol{r}_i) = \sum_{N=2} \mathcal{N}_{n_x n_y n_z}(\boldsymbol{R}_j)(n_x,n_y,n_z)_{\rm ho} \tag{B7}$$

$$+ \mathcal{O}(|\boldsymbol{R}_j|^3). \tag{B8}$$

This means that the $^{16}\mathrm{O} + p + n$ cluster model wave function becomes an $(sd)^2$ configuration of the H.O. shell-model wave function in the small $|\boldsymbol{R}_j|$ limit.

[1] A. L. Goodman, in *Advances in Nuclear Physics*, edited by J. W. Negele and E. Vogt, Vol. 11 (Plenum Press, New York, 1979), p. 263.
[2] A. L. Goodman, Phys. Rev. C **60**, 014311 (1999).
[3] P. Van Isacker, Int. J. Mod. Phys. E **22**, 1330028 (2013).
[4] W. Satula, J. Dobaczewski, W. Nazarewicz, and M. Rafalski, Phys. Rev. Lett. **103**, 012502 (2009).
[5] A. Gezerlis, G. F. Bertsch, and Y. L. Luo, Phys. Rev. Lett. **106**, 252502 (2011).
[6] K. Sato, J. Dobaczewski, T. Nakatsukasa, and W. Satuła, Phys. Rev. C **88**, 061301(R) (2013).
[7] N. Sandulescu, D. Negrea, and C. W. Johnson, Phys. Rev. C **86**, 041302 (2012).
[8] N. Sandulescu, D. Negrea, J. Dukelsky, and C. W. Johnson, Phys. Rev. C **85**, 061303 (2012).
[9] A. O. Macchiavelli, P. Fallon, R. M. Clark, M. Cromaz, M. A. Deleplanque, R. M. Diamond, G. J. Lane, I. Y. Lee *et al.*, Phys. Rev. C **61**, 041303 (2000).
[10] J. Engel, K. Langanke, and P. Vogel, Phys. Lett. B **389**, 211 (1996).
[11] W. Satula and R. Wyss, Phys. Lett. B **393**, 1 (1997).
[12] A. Poves and G. Martinez-Pinedo, Phys. Lett. B **430**, 203 (1998).

[13] A. L. Goodman, Phys. Rev. C **58**, R3051 (1998).
[14] K. Kaneko and M. Hasegawa, Phys. Rev. C **69**, 061302 (2004).
[15] S. Baroni, A. O. Macchiavelli, and A. Schwenk, Phys. Rev. C **81**, 064308 (2010).
[16] G. F. Bertsch and Y. Luo, Phys. Rev. C **81**, 064320 (2010).
[17] H. Sagawa, Y. Tanimura, and K. Hagino, Phys. Rev. C **87**, 034310 (2013).
[18] G. F. Bertsch and S. Baroni, arXiv:0904.2017 [nucl-th].
[19] K. Nichols and R. A. Sorensen, Nucl. Phys. A **309**, 45 (1978).
[20] K. Muhlhans, E. M. Muller, K. Neergard, and U. Mosel, Phys. Lett. B **105**, 329 (1981).
[21] K. Kaneko and J.-y. Zhang, Phys. Rev. C **57**, 1732 (1998).
[22] J. Terasaki, R. Wyss, and P. H. Heenen, Phys. Lett. B **437**, 1 (1998).
[23] A. L. Goodman, Phys. Rev. C **63**, 044325 (2001).
[24] M. Hasegawa, K. Kaneko, and T. Mizusaki, Phys. Rev. C **70**, 031301 (2004).
[25] B. Cederwall, F. G. Moradi, T. Back, A. Johnson, J. Blomqvist, E. Clement, G. de France, R. Wadsworth *et al.*, Nature (London) **469**, 68 (2011).
[26] S. Zerguine and P. Van Isacker, Phys. Rev. C **83**, 064314 (2011).
[27] C. Qi, J. Blomqvist, T. Back, B. Cederwall, A. Johnson, R. J. Liotta, and R. Wyss, Phys. Rev. C **84**, 021301 (2011).
[28] Y. Tanimura, H. Sagawa, and K. Hagino, Prog. Theor. Exp. Phys. **2014**, 53D02 (2014).
[29] S. Fujimoto, Phys. Rev. B **79**, 220506(R) (2009).
[30] A. B. Volkov, Nucl. Phys. **74**, 33 (1965).
[31] N. Yamaguchi, T. Kasahara, S. Nagata, and Y. Akaishi, Prog. Theor. Phys. **62**, 1018 (1979); R. Tamagaki, *ibid.* **39**, 91 (1968).
[32] T. Matsuse, M. Kamimura, and Y. Fukushima, Prog. Theor. Phys. **53**, 706 (1975).
[33] N. J. Stone, At. Data Nucl. Data Tables **90**, 75 (2005).
[34] D. R. Tilley, H. R. Weller, C. M. Cheves, and R. M. Chasteler, Nucl. Phys. A **595**, 1 (1995).
[35] Y. Taniguchi, M. Kimura, and H. Horiuchi, Prog. Theor. Phys. **112**, 475 (2004).
[36] Y. Kanada-En'yo, Phys. Rev. C **71**, 014303 (2005).
[37] N. Itagaki, H. Masui, M. Ito, and S. Aoyama, Phys. Rev. C **71**, 064307 (2005).